Hindawi Publishing Corporation
Journal of Nanomaterials
Volume 2015, Article ID 273720, 20 pages
http://dx.doi.org/10.1155/2015/273720

Review Article

High Performance Electrocatalysts Based on Pt Nanoarchitecture for Fuel Cell Applications

Young-Woo Lee,[1] SeungNam Cha,[1] Kyung-Won Park,[2] Jung Inn Sohn,[1] and Jong Min Kim[1]

[1]*Department of Engineering Science, University of Oxford, Oxford OX1 3PJ, UK*
[2]*Department of Chemical Engineering, Soongsil University, Seoul 156-743, Republic of Korea*

Correspondence should be addressed to Kyung-Won Park; kwpark@ssu.ac.kr and Jung Inn Sohn; junginn.sohn@eng.ox.ac.uk

Received 12 January 2015; Revised 10 March 2015; Accepted 10 March 2015

Academic Editor: Yong Ding

Fuel cells, converting chemical energy from fuels into electricity directly without the need for combustion, are promising energy conversion devices for their potential applications as environmentally friendly, energy efficient power sources. However, to take fuel cell technology forward towards commercialization, we need to achieve further improvements in electrocatalyst technology, which can play an extremely important role in essentially determining cost-effectiveness, performance, and durability. In particular, platinum- (Pt-) based electrocatalyst approaches have been extensively investigated and actively pursued to meet those demands as an ideal fuel cell catalyst due to their most outstanding activity for both cathode oxygen reduction reactions and anode fuel oxidation reactions. In this review, we will address important issues and recent progress in the development of Pt-based catalysts, their synthesis, and characterization. We will also review snapshots of research that are focused on essential dynamics aspects of electrocatalytic reactions, such as the shape effects on the catalytic activity of Pt-based nanostructures, the relationships between structural morphology of Pt-based nanostructures and electrochemical reactions on both cathode and anode electrodes, and the effects of composition and electronic structure of Pt-based catalysts on electrochemical reaction properties of fuel cells.

1. Introduction

Low temperature fuel cells based on the proton exchange membrane fuel cells (PEMFCs) and direct alcohol fuel cells (DAFCs) technology continue to be of considerable interest as one of the most promising electrochemical conversion devices for widespread use as clean, renewable, and non-polluting power sources in electrical vehicles and portable electronic devices as well as various stationary power systems as they offer high efficiency, modularity, low operating temperature, and low pollutant emissions [1, 2]. However, despite these attractive features and environmentally favorable energy sources with a variety of practical applications, there are challenging important issues to be addressed in order to take fuel cell technology forward towards successful commercialization. In particular, an electrocatalyst, serving as a basis for operation of fuel cells, is extremely important as a crucial component, essentially determining cost-effectiveness, performance, and durability [3].

Among various electrocatalysts studied so far, platinum- (Pt-) based electrocatalyst materials have attracted extensive attention over the past decade as an ideal fuel cell catalyst due to their most outstanding activity for both cathode oxygen reduction reactions (ORRs) and anode fuel oxidation reactions [4–6]. However, Pt catalysts still suffer from several problems, which need to be solved, such as their high cost, catalyst deactivation through active site blocking caused by CO poisoning generated as reaction by-products, and the kinetic limitation of the ORR as well as high overpotential and low long-term stability of oxygen electroreduction reactions [7–10]. To date there have been significant worldwide efforts to address such problems by introducing various architectures of Pt catalysts: (1) the shape-controlled Pt-based nanostructure [11, 12], (2) the dimension-controlled Pt-based nanostructures [13, 14], (3) the simply alloying of Pt crystal structure with a second transition metal (Co, Fe, Ni, etc.) [15–17], and (4) the bimetallic Pt-based nanostructures with core-shell structure [18, 19]. Recently, most researches

have mainly focused on control over the morphology and composition of Pt-based nanostructures to enhance their electrocatalytic activity and stability as genuinely practical approaches for fuel cell electrocatalysts [20–22]. To this end, various strategies have been developed to control the shape of Pt-based nanostructures using different synthetic routes, for example, use of polyol in aqueous or organic solution, thermal-decomposition process, and electrochemical and photochemical reduction techniques [23–27]. Furthermore, the synthesis of diverse Pt-based nanostructures has also been demonstrated by controlling the morphology and composition of catalytic nanostructures to fundamentally understand their catalytic activity and performance with their dimensional (D) versatility, such as 0D (cube, octahedron, truncated cube, and icosahedron) [28–31], 1D (wire and rod) [32, 33], 2D (plate and disk) [34, 35], and 3D nanostructures (star, flower, and dendrite) [36, 37]. In this paper, therefore, we aim to review the practical issues and recent research progress in the development of synthetic methods for high efficient, stable electrocatalysts based on nanoarchitectured Pt with various shapes and faceted morphologies. In addition, in order to understand fundamental electrochemical reaction features in low temperature fuel cells, we will focus on the following essential dynamics aspects of electrocatalytic reactions: (1) shape effects on the catalytic activity of Pt-based nanostructures, (2) relationships between structural morphology of Pt-based nanostructures and electrochemical reactions on both electrodes, and (3) effects of composition and electronic structure of Pt-based catalysts on electrochemical reaction properties of fuel cells. This review will provide insights not only into comprehensively understanding electrochemical mechanism and characteristics in fuel cell reactions, but also into developing novel and practical electrocatalysts useful for both electrode reactions in low temperature fuel cells.

2. Synthesis of Pt-Based Nanostructures as Electrocatalysts

2.1. Polyol Method in an Aqueous or Organic Solution. A polyol approach, which is an effective technique to synthesize particles with a wide range of sizes and morphologies, has attracted attention for the induced reduction of a metal precursor due to the easy and cost-effective synthetic method. This method is based on the decomposition of alcohol containing hydroxyl (–OH) functional groups and the proposed basic reduction mechanism in ethylene glycol as a reducing agent is as follows [38]:

$$2CH_2OH\text{–}CH_2OH \longrightarrow 2CH_3\text{–}CHO + 2H_2O \quad (1)$$

$$2CH_3\text{–}CHO + \text{Me ion} \longrightarrow CH_3CO\text{–}CH_3CO + \text{Me}\,(0) + H_2O \quad (2)$$

Here it is important to note that the kinetic rates of reduction of metal ions, affecting the morphology and shape of particles, can be strongly influenced by alky chain lengths, which are different depending on employed reducing agents, such as ethylene glycol, L-ascorbic acid, citric acid, and poly(vinyl pyrrolidone) (PVP) [39]. Xia group reported that truncated octahedrons (or the so-called Wulff polyhedron) enclosed by eight {111} and six {100} facets of Pd can be obtained from the L-ascorbic acid, exhibiting a fast kinetic rate (Figure 1(b)) [40]. Also, when the citric acid with a moderate kinetic rate of reduction was used as a reducing agent, the icosahedrons, octahedrons, and decahedrons of Pd enclosed by the {111} facets were obtained, as shown Figure 1(c). In contrast, the PVP with a long alkyl chain and two hydroxyl groups at end group of polymer exhibits much low kinetic rate of reduction. As a result, the Pd nanostructures with the shape of hexagonal and triangular nanoplates were synthesized by using PVP because their nuclei with a metastable hexagonal structure could remain small for a long period of time due to the slow addition of atoms, gradually evolving into plate-like seeds in Figure 1(d).

In recent, we synthesized the Pt-Pd nanostructure with an octahedral shape enclosed by {111} facets using glycerol as a new reducing agent in aqueous solutions [41]. It was found that the glycerol can lead to the faster reduction reaction of metal ions because it has a relatively short alkyl chain and three hydroxyl groups. Moreover, it is believed the fast reduction reaction might tend to thermodynamically minimize crystalline surface energy and hence resulting in the formation of crystal facets with the lower surface energy in the structure. Thus, this implies that Pt-Pd nanostructure can be synthesized with {111} side facets, forming the octahedral shape by the rapid reduction reaction due to the relative surface energy of $\gamma\{111\} < \gamma\{100\} < \gamma\{110\}$ planes in *fcc* structures [42]. Furthermore, to confirm reduction mechanism by glycerol, we performed Fourier transform infrared (FT-IR) measurements. In general, according to the basic mechanism of metal reduction induced by the polyol, metal ions are reduced to metal atoms by an aldehyde (CHO) functional group, which is transformed into a carboxyl (COOH) group with a ketone (C=O) group. Thus, as a strong evidence of oxidized glycerol, the IR absorption band of the C=O stretch was clearly observed between 1720 and 1740 cm^{-1} in Figure 2(a). This finding clearly confirmed that the glycerol was changed into glyceraldehydes and glyceric acid during the reduction of metal ions as shown in Figure 2(b).

In addition, it has been also reported that additive agents, such as organic materials like polymer and small molecules acting as capping agents, metal ions with redox potential, and halogen ions, play an important role in controlling the shape of Pt-based nanostructures. For example, organic materials, such as PVP, cetyltrimethylammonium-bromide (CTAB) and chloride (CTAC), citrate, sodium polyacrylate, tetradecyltrimethylammonium bromide (TTAB), effectively act as both a surface adsorption agent for shape-controlled nanoparticles and a surfactant agent for prevention of aggregation among metal nanoparticles during synthesis process [43–46]. However, although organic materials are beneficial for the shape control of the metal, they often exhibit a reduced or poisoning phenomenon of active sites in the electrochemical reactions due to the strong chemical adsorption between capping agents and catalyst surface. Thus, for electrochemical applications in fuel cells, it is essentially imperative to remove organic capping agents from catalyst surface. For this, various strategies have been

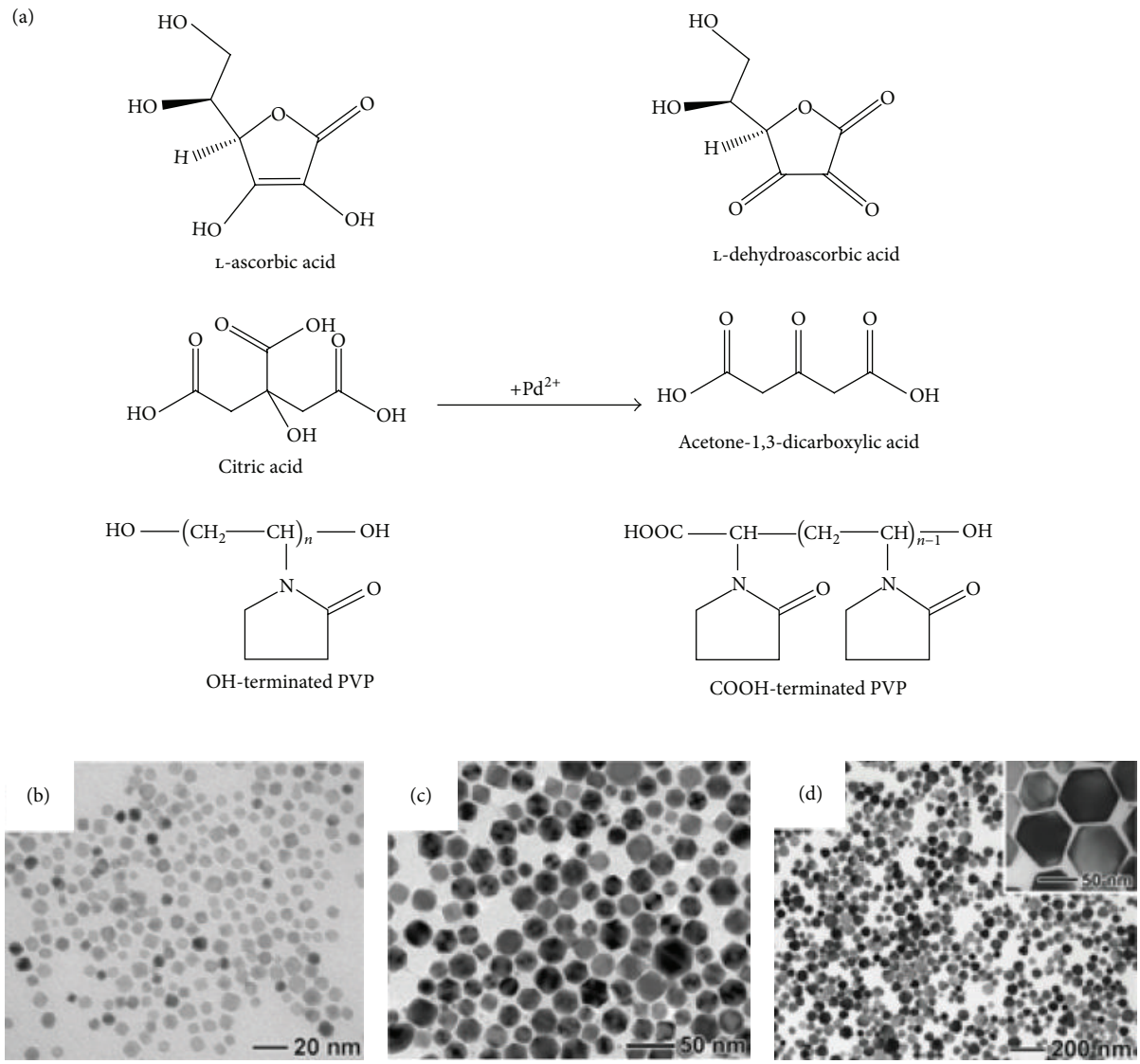

FIGURE 1: (a) Structural illustration of L-ascorbic acid, citric acid, and OH-terminated PVP and their oxidized forms due to the redox reactions with Pd^{2+} ions. TEM images of Pd (b) truncated octahedrons, (c) icosahedrons, and (d) hexagonal and triangular nanoplates synthesized by L-ascorbic acid, citric acid, and PVP, respectively. Reproduced with permission from [40].

developed by using different techniques, such as acid [47], thermal [48], UV-ozone [49], electrochemical [50], plasma [51], or chemical treatment [52]. However, whereas these approaches have advantages of a relatively high removal rate for organic capping agents, these cause the formation of secondary defects on catalyst surface and the variation of an as-prepared Pt-based nanostructure shape. Accordingly, the advanced development of effective surface treatment process and synthesis methods based on nonorganic capping agents is required for enhanced electrochemical properties in low temperature fuel cells.

In addition to introduction of various reducing agents with different alky chain lengths and organic capping agents for the control of Pt-based nanostructure shapes, utilizing metal cations, such as Fe^{2+}/Fe^{3+} and Ag^{+} ions, and even nonmetal anions, such as NO_3^{-}, can be considered as another strategy to adjust the shape of Pt-based nanostructures. As shown in Figure 3, Song and coworkers demonstrated the synthesis of Pt nanostructures with the controlled shape by the selective adsorption of Ag ions as an additive agent [53]. As the concentration of Ag ions in reaction solution is continuously increased, the shape of Pt nanostructures is changed from cube to octahedron. We also demonstrated the growth of cubic Pt nanostructures using Fe^{2+}/Fe^{3+} ions having redox potential as an additive agent [54]. Fe^{3+} ions could lead to slow nucleation and growth of Pt, leaving behind thermodynamically stable {100} planes. That is, Fe^{3+} ions can greatly reduce the supersaturation of Pt atoms, resulting in formation of a stable crystal plane. The growth dynamics of Pt nanocubes can be described by the following equation:

$$2Fe^{3+} + Pt^{0} \longrightarrow 2Fe^{2+} + Pt^{2+} \quad (3)$$

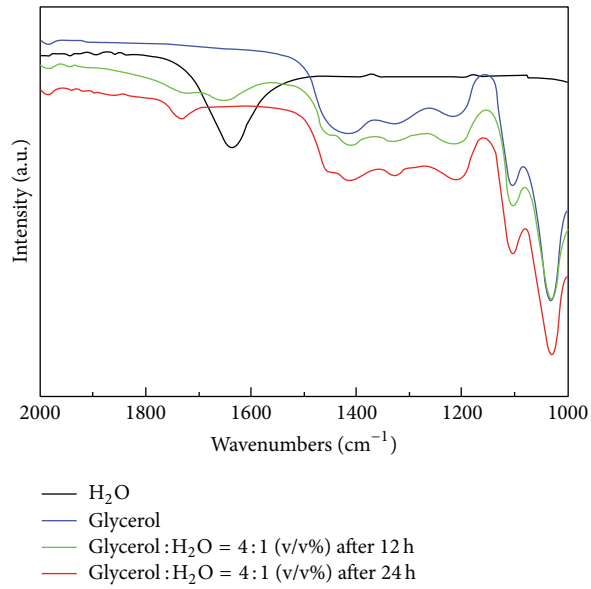

(a)

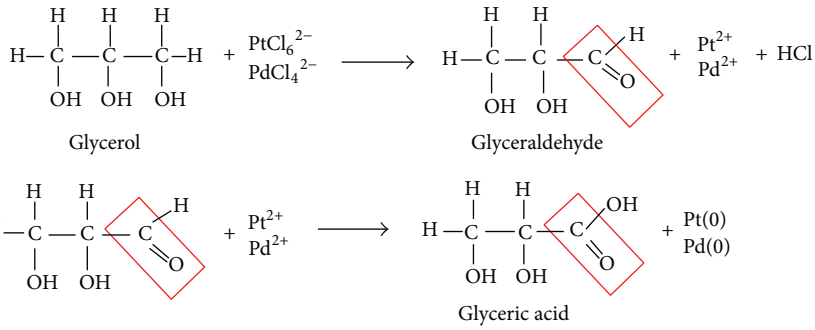

(b)

Figure 2: (a) FT-IR spectrum with respect to the reduction of metal salts with glycerol as a reducing agent in aqueous solution at 12 and 24 h in comparison with H_2O. (b) The reduction mechanism of Pt and Pd ions for Pt-Pd alloy nanoparticles synthesized using glycerol as a reducing agent. Reproduced with permission from [41].

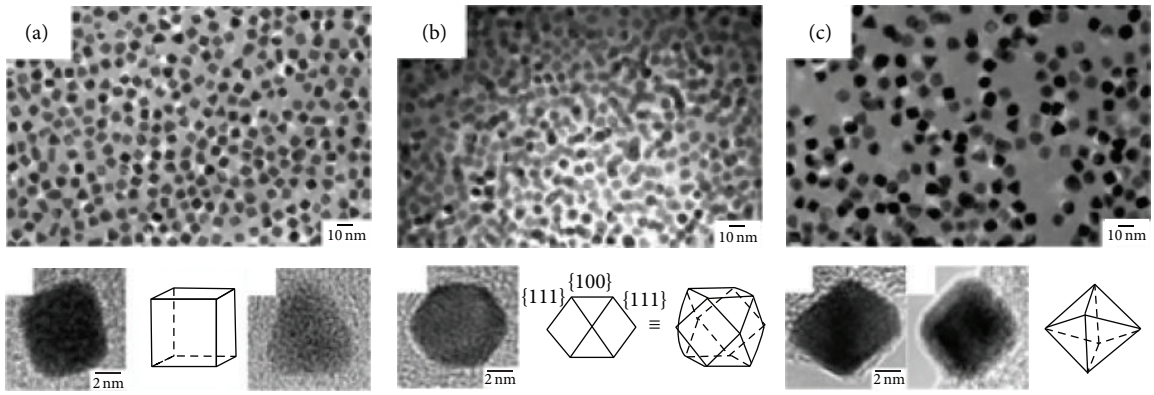

Figure 3: TEM and HR-TEM images of Pt (a) cube, (b) cuboctahedron, and (c) octahedron resulting from different Ag concentrations in solution during growth. A mole fraction of Ag to Pt in cube, cuboctahedron, and octahedron is 1.1, 11, and 32 mol%, respectively. Reproduced with permission from [53].

Similar to roles of Ag^+ ions in nanoparticle growth, Xia and coworkers reported that a variety of shapes in Pt-based nanostructures can be obtained through the control of kinetic reduction rates by NO_3^- ions as an additive agent [55]. It was found that Pt nanoparticles exhibited an irregular shape and their sizes varied in the range of 3–5 nm without the introduction of NO_3^- ions. Noticeably, as the molar concentration of NO_3^- ions was increased, the geometrical morphology of Pt nanoparticles was transformed from an irregular shape with smaller size, through a polyhedral shape with uniform size until 3.3 molar ratios of NO_3^- ion to Pt salt, to the uniform octapod and tetrapod at high concentration of NO_3^- ions over 3.3 molar ratios. These results indicate that NO_3^- ions could hinder the reduction of Pt(IV) ions because the reduction potential of NO_3^- ion is higher than that of Pt(IV) ions as follows:

$$NO_3^- + 2H^+ + 2e^- \longrightarrow NO_2^- + H_2O \quad E^\circ = 0.94\,V \quad (4)$$

$$PtCl_6^{2-} + 2e^- \longrightarrow PtCl_4^{2-} + 2Cl^- \quad E^\circ = 0.74\,V \quad (5)$$

They also confirmed the formation of intermediate $Pt(NO_2)_6^{2-}$ ions. This finding suggests that $Pt(NO_2)_6^{2-}$ ions can play a role in reducing the rate of reduction during the synthesis process.

2.2. Thermal-Decomposition Method. Compared to a polyol method, a thermal-decomposition approach is beneficial for the production of shape-controlled Pt-based nanostructures with high yield, uniform shape, and high reproducibility because of protection from oxidative etching and subreaction [56, 57]. Furthermore, it is recognized that this is a very effective method for designing core@shell structures and controlling alloy compositions.

Recently, we reported that Pt nanocubes were successfully synthesized by a thermal-decomposition method using PVP as an additive agent, 1-octadecene as a solvent, and oleylamine as a capping agent for enhanced electrochemical properties in alcohol electrooxidation reactions [31]. It is worth noting that the shape controlled Pt-based nanostructure with not only unique exposed surface, but also large surface area is important to enhance the electrochemical properties. However, it has been mostly reported that Pt-based nanostructures with shape control have lager particle size of over 10 nm, hence exhibiting smaller electrochemical active surface areas (EASAs). Accordingly, for enhanced electrochemical properties, the ability to tailor facets and size of Pt-based nanomaterials is tremendously important, allowing favorably exposed surface structures of nanoparticles with smaller size comparable to commercial Pt electrocatalysts. It was clearly observed that our Pt nanocubes have much smaller particle size of average 4.5 nm compared to previously reported nanocubes with particle size of over 10 nm [58, 59]. In particular, we found that PVP can play an important role in forming Pt cubes enclosed by {100} facets and monodispersed nanoparticles in Figures 4(a) and 4(b) due to its attractive feature to bind with Pt {100} facets. On the contrary, Pt nanoparticles synthesized in the absence of PVP showed the polydispersed nanoparticles and slight aggregation between nanoparticles as shown in Figure 4(c). Moreover, it has been shown that amine functional groups could be important key factors to determine the shape and size of Pt-based nanocubes through assistance of W metal ions controlling kinetic reduction rate or/and carbon monoxide (CO) gas acting as a selective adsorption material. For example, Fang and coworkers demonstrated the synthesis of PtM alloy (M is Co, Fe, and Ni) nanocubes by introducing $W(CO)_6$ in oleylamine and oleic acid solutions [60]. They suggested that the use of $W(CO)_6$ is crucial for controlling nucleation process and that an optimized ratio of oleylamine and oleic acid pair is the key to enable us to obtain the lowest total surface energy. They believed that the preferential chemisorption and monolayer adsorption of oleylamine on {100} facets of PtM can lead to the lowering of total surface energy of the {100} facet of PtM, resulting in the cube shape. Fu and coworkers also reported that Pt nanocubes can be synthesized using CO in a mixed solvent system of oleylamine and oleic. Similar to the oleylamine, it is revealed that the CO gas strongly binds with Pt {100} facets, affecting the morphology of Pt nanoparticles [61]. To further understand the role of CO in determining the shape of Pt nanoparticles, they performed calculations for change in the surface energy (γ) between the {100} and {111} facets of Pt before and after adsorption of amine and/or CO molecule using spin-polarized density functional theory (DFT). It is found that the surface energy of $\gamma_{\{100\}}$ (0.90 eV/atom) is higher than that of $\gamma_{\{111\}}$ (0.64 eV/atom) before adsorption of amine and CO molecule. Interestingly, however, the change of surface energy is significantly altered after adsorption of amine and CO molecule; that is, $\Delta\gamma_{\{100\}\text{-}\{111\}}$ is −0.02 eV/atom. This is because adsorption energy of amine and CO on Pt {100} facets is highly increased compared to Pt {111} facets. This indicates that the coadsorption of CO and amine on Pt {100} results in the formation of Pt nanocubes.

2.3. Electrochemical and Photochemical Reduction Methods. Electrochemical and photochemical reduction approaches, needing external energy for reduction reactions, have the enormous potential for the production of shape-controlled Pt-based nanostructures as they have the advantages of high yield of shape and size of Pt-based nanostructures, reproducibility, and nontoxic reaction as well as detailed understanding of formation mechanism in Pt-based nanostructures. However, there still remain difficulties in large scale production to move towards a genuinely practical technology for commercialization. In this regard, it is highly necessary to seek for a novel and simple strategy to solve such a problem.

On the basis of the electrochemical reduction technique, many studies have been performed to achieve shape-controlled Pt-based nanostructures using different electrochemical techniques, such as square-wave potential (pulse potential), and constant reduction current/potential. Typically, in the electrochemical reduction method, for the synthesis of shape-controlled Pt nanostructures the experimental setup consists of electrolyte and three electrodes, namely, working, reference, and counter electrodes. Furthermore, negative potential or current is applied for the reduction reaction from metal ions to metal atoms. In particular,

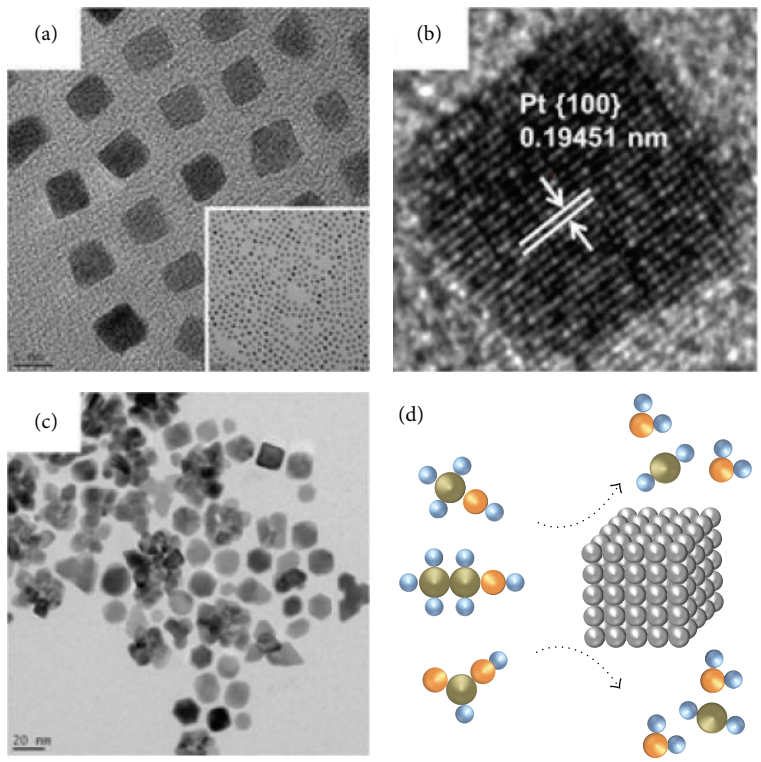

Figure 4: (a) TEM and (b) HR-TEM images of Pt nanocubes synthesized in the presence of PVP. (c) TEM image of Pt NPs synthesized in the absence of PVP. (d) Schematic diagram illustrating the alcohol (i.e., formic acid, methanol, and ethanol) electrooxidation on Pt nanocubes. Reproduced with permission from [31].

Wang and coworkers reported tetrahexahedral (THH) Pt nanostructures enclosed by high-index facets with almost {730} facets and some {210}, {310}, or {520} facets, as shown in Figure 5(b) [62]. It was found that the particle size of THH Pt nanostructures was increased with the reaction time, from 53 to 144 nm. In particular, they suggested that formation mechanism of THH Pt nanostructures based on a square-wave potential technique as follows (in Figure 5(a)). (1) At high potential (1.20 V), Pt atoms on surface of as-formed Pt nanospheres can be oxidized and partially dissolved into electrolyte, causing defects. (2) At low potential (−0.20~ −0.10 V), dissolved Pt ions diffuse to the surface of Pt crystal and then are reduced to Pt atoms. Thus, Pt atoms on the surface of low-index planes like a {111} facet with the high coordination number (CN) are readily oxidized/dissolved by the oxygen atom, which results in a structural change of the Pt surface. In contrast, in the case of high index planes with the low CN, the oxygen atoms preferentially adsorb on the high index surface sites of Pt, hence maintaining the unchanged surface structures. Also, Raoof and coworkers showed that novel Pt nanostructures can be successfully synthesized using a constant potential deposition method. As-prepared Pt nanostructures exhibited a rod-like shape with 1D structure due to the selectivity adsorption of oxygen atoms of dextrin on the Pt surface [63].

Alternatively, the photochemical reduction method was developed as a way to form noble metal nanoparticles by reducing noble metal ions in the presence of semiconducting

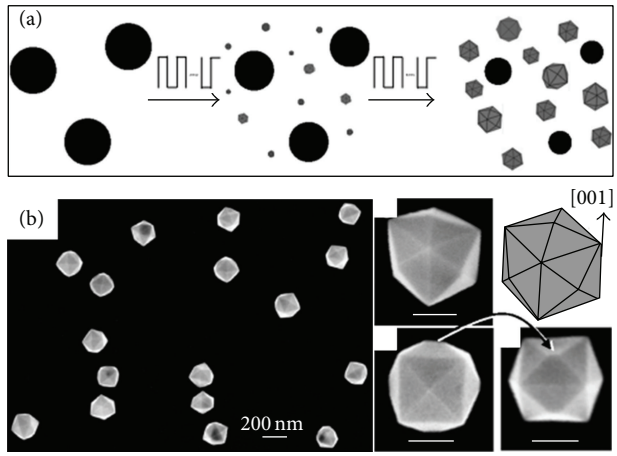

Figure 5: (a) Scheme of electrochemical preparation of the THH Pt NCs from nanospheres using square-wave potential. (b) SEM images of the THH Pt nanocrystal. Reproduced with permission from [62].

metal oxides (SMOs) such as TiO_2 and ZnO. The proposed reduction mechanism of metal (M) ions in the photochemical reduction process in the presence of the SMO materials is as follows:

$$\text{SCM} + h\nu \longrightarrow \text{SCM}\left(\text{h}^+ + \text{e}^-\right) \tag{6}$$

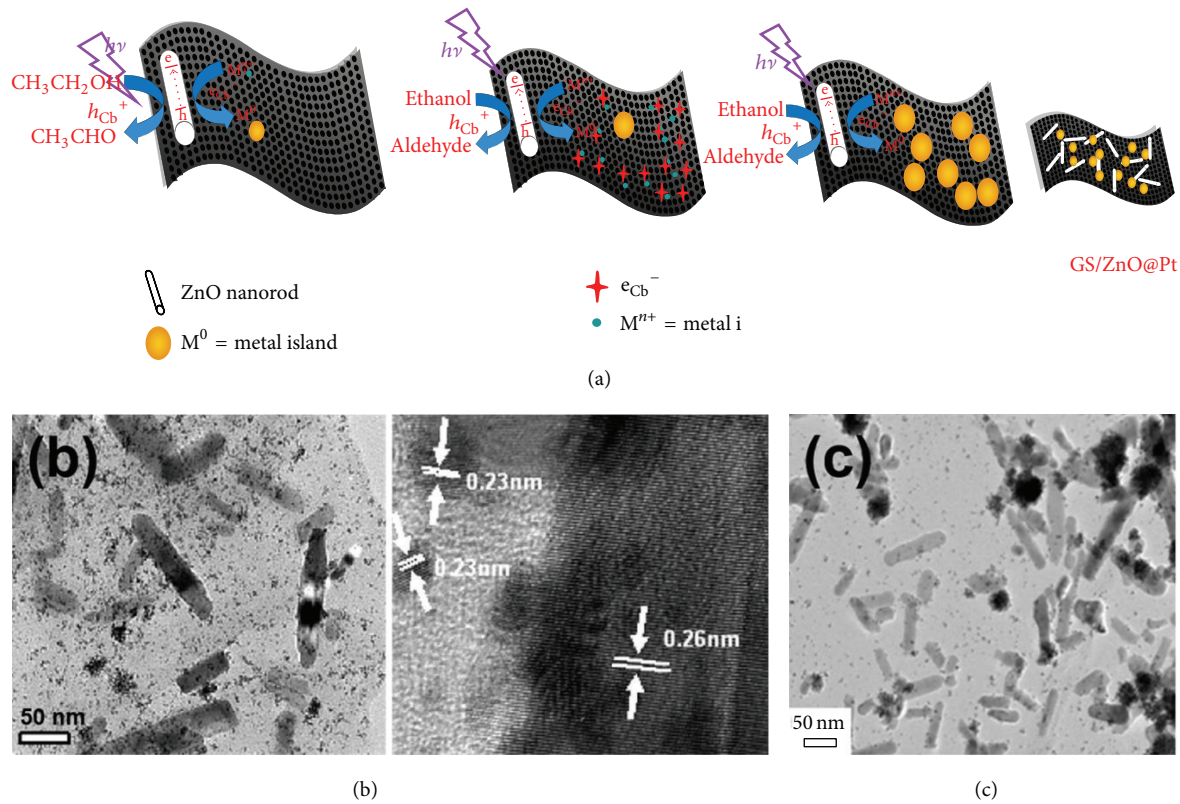

FIGURE 6: (a) Schematic illustration for procedures of ZnO@Pt deposited on graphene sheets (GS/ZnO@Pt) nanostructures using photochemical reduction method. TEM images of GS/ZnO@Pt nanostructures prepared by difference amount of metal ions: (b) 380 μL and (c) 580 μL. Reproduced with permission from [64].

$$\mathrm{SCM}\left(e^{-}\right) + M^{+} \longrightarrow \mathrm{SCM} + M \quad (7)$$

$$\mathrm{SCM}\left(2h^{+}\right) + C_2H_5OH \longrightarrow \mathrm{SCM} + 2H^{+} + CH_3CHO \quad (8)$$

As shown in the above reaction equations, when light (energy, $h\nu$) is irradiated into a reactor, electron, and hole pairs are generated in SMOs (equation (6)). The generated electrons participate in the reduction of M ions (equation (7)), while the holes are used to oxidize ethanol, which is an additive agent (equation (8)).

Recently, Gu and coworkers developed an alternative method for the synthesis of ZnO@Pt nanoparticles using the UV irradiation of an ethanolic solution containing H_2PtCl_6 and ZnO deposited on graphene sheet as shown in Figure 6 [64]. Also, it has been reported that various M@TiO_2 nanoparticles (M = Ag, Pd, Au, Pt) can be synthesized using the photochemical reduction process [65, 66]. Furthermore, Huang and coworkers demonstrated the synthesis of shape-controlled Au nanoparticles with six star using photoirradiation of an ethanolic solution containing $HAuCl_4$ and TiO_2 sols without the addition of any other surface capping molecules [67]. Thus, these findings suggest that a photochemical reduction method based on the reduction mechanism of metal ions can be one of the viable ways to achieve Pt nanostructures with controlled size and shape.

For the further comparison of three different synthetic methods, we summarize the advantages and disadvantages of each synthesis approach for the shape-controlled Pt-based nanostructures in Table 1.

3. Electrochemical Reactions of Pt-Based Nanostructures in Low-Temperature Fuel Cells

In general, low-temperature fuel cells, such as PEMFCs and DAFCs, consist of two electrodes with one anode and the other cathode separated by a membrane (so-called MEA: membrane electrode assembly), gas diffusion layer, and bipolar plate in an unit cell as shown in Figure 7. In particular, DAFCs are also classified as direct formic acid, direct methanol, and direct ethanol fuel cells according the type of fuels. Their basic electrochemical reactions involve the electrooxidation reaction of fuels taking place at the anode and the electroreduction reaction of oxygen occurring at the cathode. Therefore, to enhance electrochemical properties in both electrodes, there have been many efforts to manipulate the shape and composition of Pt-based nanostructures as electrocatalysts for fuel cells. In this section, we will review the fuel electrooxidation and oxygen electroreduction reactions and will discuss the detailed electrochemical correlation

Table 1: Comparison of various synthetic methods.

Methods	Advantages	Disadvantages
Polyol	(1) Large quantity production (2) High reproducibility (3) Low temperature condition	(1) Moderate shape and size yield (2) Difficult to remove capping agents
Thermal-decomposition	(1) Large quantity production (2) High shape and size yield (3) High reproducibility	(1) Difficult to remove capping agents (2) High temperature condition (3) Non-air condition (4) Use toxic solvent and many additive agents
Photochemical	(1) High shape and size yield (2) Environmentally friendly	(1) Difficult for large quantity production (2) Unclear growth mechanism (3) Required many subdevices and part
Electrochemical	(1) High shape and size yield (2) Environmentally friendly (3) High reproducibility	(1) Difficult for large quantity production (2) Required many subdevices and part

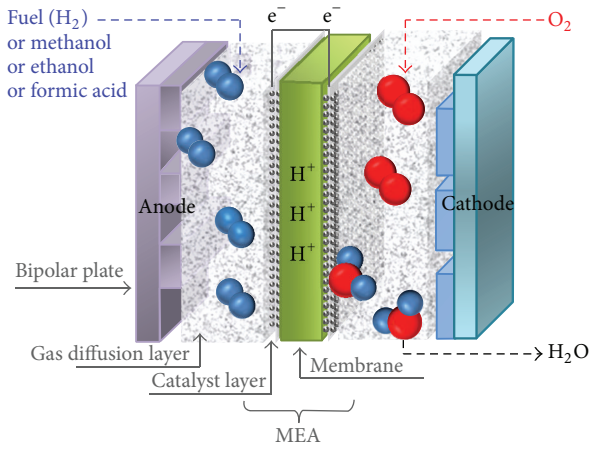

Figure 7: Schematic illustration of low-temperature fuel cells.

between each reactant and Pt-based nanostructures associated with their morphology and composition.

3.1. Fuel Electrooxidation Reaction. In direct formic acid fuel cells (DFAFCs), the anodic reaction considered as the most important reaction is the formic acid oxidation reaction (FAOR). It has been well known that Pt-based materials are the most effective electrocatalyst for FAOR. However, Pt and Pt-based catalysts suffer from the catalyst deactivation process caused by CO poisoning, one of the most crucial issues, as CO-species generated as a by-product of the formic acid electrooxidation reaction disturb electrochemical reactions by blocking active sites. There are two possible routes for formic acid electrooxidation reactions as follows:

$$\text{Direct pathway: HCOOH} \longrightarrow \text{HCOO}_{ad} \longrightarrow \text{CO}_2 + \text{H}^+ + \text{e}^- \quad (9)$$

$$\text{Indirect pathway: HCOOH} \longrightarrow \text{CO}_{ad} + \text{H}_2\text{O} \longrightarrow \text{CO}_2 + 2\text{H}^+ + 2\text{e}^- \quad (10)$$

Here it is noted that, in the direct oxidation pathway, the formic acid is perfectly oxidized to carbon dioxide without reaction intermediates, while, in the indirect pathway, the CO-species are generated as intermediate species, which strongly adsorb onto the Pt catalyst and hence resulting in reducing the active surface area. Thus, recently, there have been enormous efforts to overcome the CO poisoning-induced catalyst deactivation process and to enhance the oxidation rate of formic acid on metallic catalysts by introducing alloying Pt with other highly oxophilic metals and/or shape-controlled Pt nanostructures to induce either electrooxidation of adsorbed intermediate species or the direct oxidation pathway [18, 22, 93].

Recently, it has been demonstrated that Pt- or Pd-based catalysts for FAOR exhibit the enhanced electrochemical properties such as lower on-set potential and higher current density than other catalysts and that surface structure or lattice parameter of catalysts plays a major role for the enhanced electrocatalytic activity due to the bridge-bonded adsorbed formate on catalyst surface in the formic acid electrocatalytic oxidation [94]. Based on these findings, we developed Pt-Ni alloy nanostructures for formic acid electrooxidation by using a thermal-decomposition method [95]. Note that as the lattice parameter of Pt (3.939 Å) is larger than that of pure Pd (3.893 Å), we selected Ni (3.523 Å) to modulate the lattice parameter of Pt-based crystal similar to that of pure Pd as shown in Figure 8(c). It was observed that the Pt-Ni alloy nanostructures show dendritic shapes (Figure 8(a)) and that the lattice parameter of Pt_3Ni_1 alloy (3.898 Å) is similar to that of pure Pd. Thus, as expected, the Pt_3Ni_1 alloy nanodendrites exhibited higher current density than commercial Pt at first anodic peak, which means the complete oxidation of formic acid, because of a well-defined alloy formation between Pt and Ni as well as high surface area of dendritic shapes, as shown in Figure 8(b).

Alternatively, it has been often reported that Pt-based nanostructures with high-index facets can be considered as efficient electrocatalysts for FAOR due to their exposed surface structure with a large amount of atomic steps. Huang and coworkers reported that concave polyhedral Pt nanocrystals exhibit 5.57 times higher current density than that in

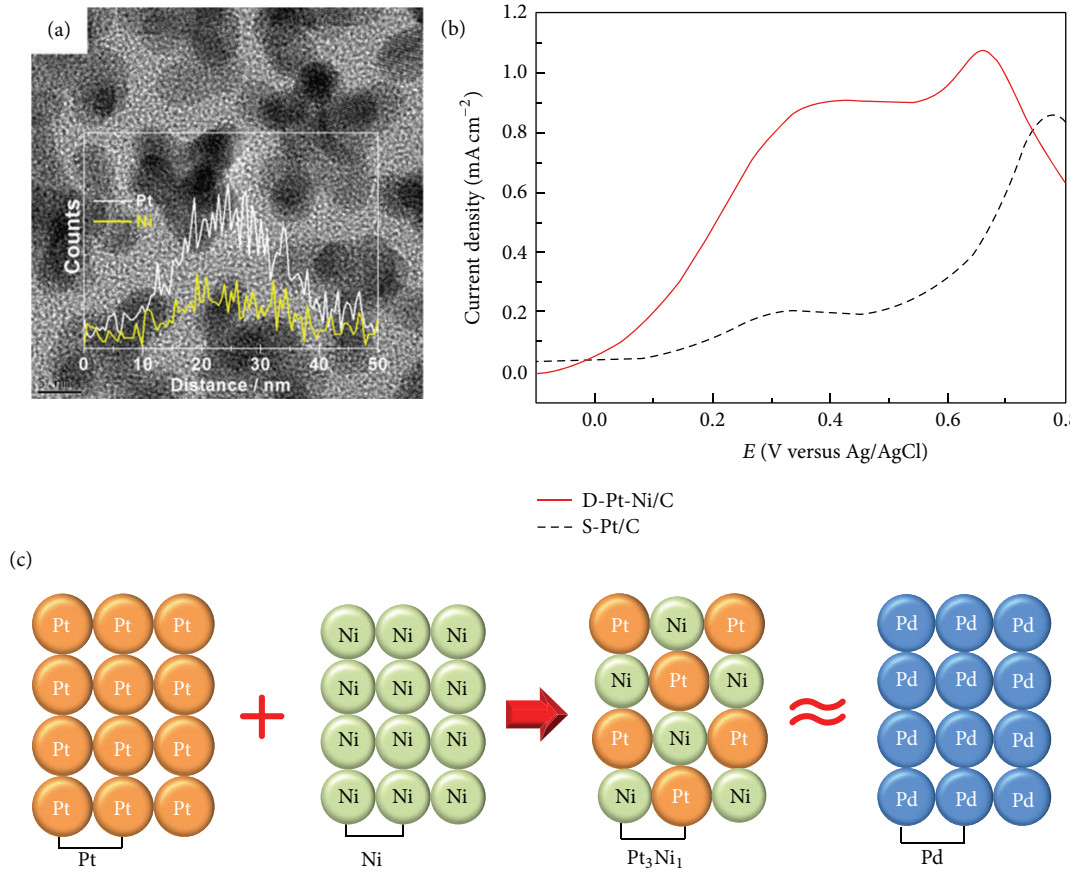

FIGURE 8: (a) FE-TEM image of the Pt_3Ni_1 alloy nanodendrites. The inset shows a line scanning profile across a Pt-Ni nanodendite. (b) Formic acid electrooxidation curves of Pt_3Ni_1 alloy nanodendrites and commercial Pt. (c) Relationship of lattice parameters of Pt, Ni, Pd, and Pt_3Ni_1. Reproduced with permission from [95].

commercial Pt due to higher density of atomic step on a {411} high-index facet as shown in Figure 9 [96]. Furthermore, Solla-Gullón and coworkers demonstrated comparison of electrochemical properties between modulated Pt nanostructures with different index facets [97]. It has been clearly found that the FAOR activity is significantly dependent on facets of Pt nanostructures, exhibiting quite different FAOR activity as follows: {111} > mixed{100}–{111} > {100} facets.

Similar to FAOR, CO-poisoning, primarily for Pt catalyst deactivation, is a crucial problem in the methanol oxidation reaction (MOR). Thus, many recent efforts have been focused on the deterioration of CO poisoning to enhance the oxidation rate of methanol by alloying Pt with 2nd metallic elements (M^{2nd}) based on high oxophilic metals, such as Ru, Pd, Ni, and Cu, favorably adsorbing hydroxyl species and then facilitating to oxide the adsorbed CO. Thus, it is expected that Pt-based alloy nanostructures with 2nd metallic elements can excellently enhance the electrocatalytic activity due to a bifunctional effect between both Pt and 2nd metal forming an alloy and the downshift of the d-band center of the pure Pt electronic structure, resulting in oxidizing the CO-species during the reactions. The bifunctional electrocatalytic mechanism for CO-species oxidation is proposed as follows:

$$\mathrm{Pt} + \mathrm{CH_3OH} \longrightarrow \mathrm{Pt{-}CO} + 4\mathrm{H^+} + 4\mathrm{e^-} \quad (11)$$

$$\mathrm{M^{2nd}} + \mathrm{H_2O} \longrightarrow \mathrm{M^{2nd} - OH} + \mathrm{H^+} + \mathrm{e^-} \quad (12)$$

$$\mathrm{Pt{-}CO} + \mathrm{M^{2nd} - OH} \longrightarrow \mathrm{Pt} + \mathrm{M^{2nd}} + \mathrm{CO_2} + \mathrm{H^+} + \mathrm{e^-} \quad (13)$$

Alternatively, on the basis of bifunctional electrocatalyst techniques, the development of shape-controlled nanoparticles with high specific catalyst surface (i.e., dendritic, star, and multipod shape) and/or exposed high active facets is also of particular interest for the enhanced electrochemical activity in MOR. Huang and coworker developed the synthesis of hyperbranched PtRu nanostructures using seed-mediated process at low-temperature for MOR [98]. It has been shown that hyperbranched PtRu nanostructures exhibit a high current density and fast on-set potential compared to pure Pt and PtRu black due to their high surface area and presence of Ru metals for bifunctional action. It was also clearly observed that carbonaceous intermediates, such as CO, $HCOO^-$, and HCO^-, were completely removed, indicating that methanol can be perfectly oxidized during the reaction. Moreover, Yang and coworkers developed Pt-Cu alloy concave nanocubes with high-index facets for MOR [99]. They observed that the Pt-Cu alloy concave nanocubes exhibit the enhanced electrochemical properties, that is, 4.7 times higher current

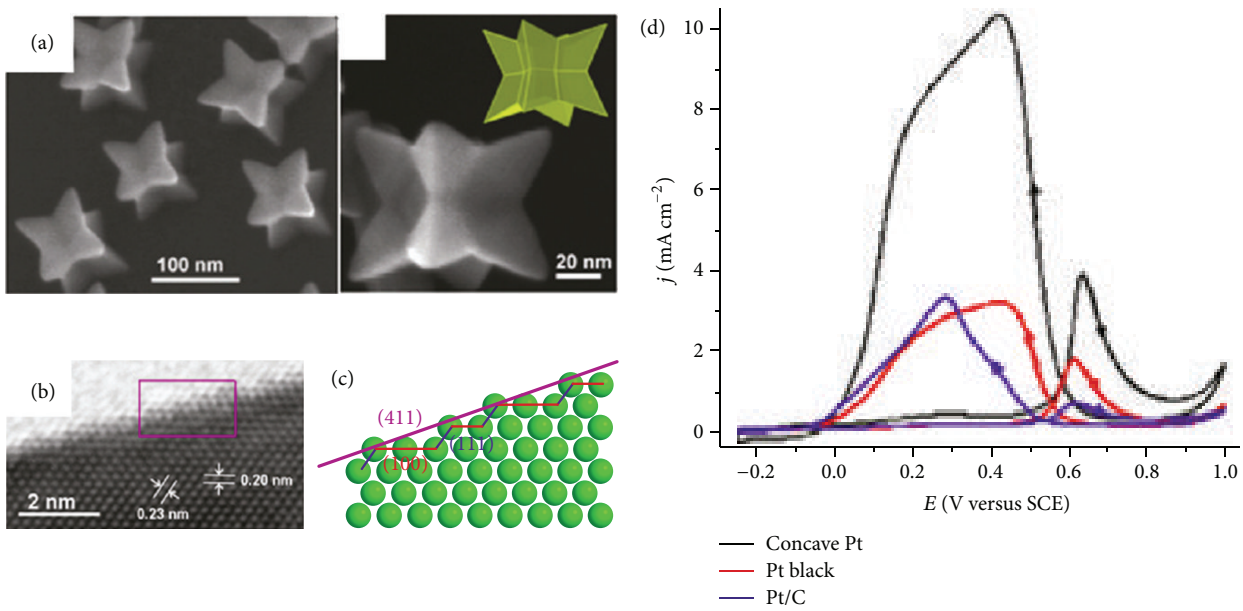

Figure 9: (a) SEM images and (b) HR-TEM image of the concave Pt nanocrystals. (c) Atomic model of {411} facet. (d) CV curves for electrooxidation of formic acid. Reproduced with permission from [96].

density, compared to commercial Pt, because the Cu atoms in Pt-Cu alloy nanostructures might induce the downshift of the d-band center of the pure Pt electronic structure and bifunctional effects, causing the oxidation of CO-species. Additionally, it is noteworthy that Pt {111} facets exhibit a lower on-set potential and a higher current density compared to other low-index facets in MOR. Thus, we investigated octahedral Pt-Pd alloy nanostructures with dominantly exposed {111} facets as shown in Figure 10(b) [41]. The octahedral Pt-Pd alloy nanostructures with the elemental composition of 47.8 at% of Pt and 52.2 at% of Pd exhibited the enhanced electrocatalytic activity, that is, higher maximum current density and lower reverse current density, in comparison with commercial Pt as shown in Figure 10(c), which is believed to be attributed to the bifunctional effect based on Pd and the octahedral shape enclosed by {111} facets.

In addition to methanol, ethanol as another candidate source suitable for fuel cells has attracted attention, because it can offer relatively high theoretical mass energy density (8 kWh kg^{-1}). However, the strong C-C bonds in ethanol cause a high overpotential at an anode, resulting in cell performance deterioration. Thus, researches have been focused on the development of an effective catalyst with high electrocatalytic activity in an ethanol oxidation reaction (EOR) by modifying catalyst surface or employing other 2nd atoms to break strong C-C bonds. For example, Rao and coworkers showed that the cubic Pt-Rh alloy nanostructures have higher ethanol electrocatalytic activity as indicated in Figure 10(a) [100]. Based on electrochemical *in situ* FT-IR spectroscopic measurements, they found that Pt_9Rh_1 nanocubes showed higher electrooxidation current density in EOR compared to other nanocubes in Figure 11(b). However, interestingly, the perfect oxidation reaction rate of the Pt_9Rh_1 nanocubes in ethanol was 0.5 times lower than that of Pt_1Rh_1 nanocubes (Figure 11(c)), because the Pt_9Rh_1 nanocubes have not sufficient active sites for breaking strong C-C bonds. On the other hand, Pt_1Rh_1 nanocubes with relatively large amounts of Rh exhibited the improved conversion selectivity from ethanol to CO_2 because Rh can help easily oxidize intermediate species and break C-C bond of ethanol. This finding is consistent with results of other studies where Rh nanostructures can significantly enhance the ethanol electrooxidation activity [101].

Here, please note that it is substantially difficult to directly compare the differences in electrochemical performance among previously reported results because shape-modified Pt-based nanostructures for the diverse anodic reactions in PEMFC have been developed by using various synthesis approaches. To this end, in order to further introduce various shape-controlled Pt-based electrocatalysts, we summarize various synthesis approaches applied for enhanced electrochemical properties in typical alcohol electrooxidation reactions in Table 2.

3.2. Oxygen Electroreduction Reaction of Pt-Based Nanostructures. The ORR is a fundamental and pivotal reaction occurring at the cathode in low temperature fuel cells where molecular oxygen adsorbs to the catalyst surface and is reduced to water through the following two pathways:

$$\text{Four-electron pathway: } O_2 + 4H^+ + 4e^- \longrightarrow 2H_2O \quad E^\circ = 1.23\ \text{V} \tag{14}$$

$$\text{Two-electron pathway: } O_2 + 2H^+ + 2e^- \longrightarrow H_2O_2 \quad E^\circ = 0.70\ \text{V} \tag{15}$$

As shown in Figure 12, the ORR requires a high potential (1.23 V) for the direct four-electron pathway and usually uses

Table 2: Summary of various Pt-based nanostructures and their synthesis method with enhanced electrochemical properties in each alcohol electrooxidation for PEMFCs.

Application	Material/ shape	Synthesis method	Experimental factor	Maximum current density at 50 mV s^{-1}	Electrolyte	Reference
FAOR	Pt-Cu/hierarchical trigonal bipyramid nanoframe	Polyol	Concentration of KI	3.77[a] 0.78[b]	0.5 M H_2SO_4 + 0.25 M HCOOH	[68]
	Pt-Fe/cube	Thermal-decomposition	Presence of $W(CO)_6$	~1.6[a,c]	0.1 M $HClO_4$ + 0.5 M HCOOH	[69]
	Pt/Multipod, disc, and hexagon	Electrochemical deposition	Reduction potential	0.017[a] (multipod) 0.01[a] (disc) 0.03[a] (hexagon)	0.5 M H_2SO_4 + 0.25 M HCOOH	[70]
	Pt_1Au_3/nanotube	Polyol/galvanic replacement process	Ag nanotemplate	1.4[b]	0.5 M H_2SO_4 + 0.5 M HCOOH	[71]
	Pt/trapezohedron	Electrochemical deposition	Square-wave potential	4.1[a]	0.1 M $HClO_4$ + 0.25 M HCOOH	[72]
MOR	Pt-Ag/octahedron	Polyol	Selective oxidative etching on Ag^0	2.96[a] ~0.35[b]	0.5 M H_2SO_4 + 1.0 M CH_3OH	[73]
	Cu@PtCu/hexagonal shape	Polyol	Presence of Fe^{3+} ion	1.77[a] 0.889[b]	0.5 M H_2SO_4 + 1.0 M CH_3OH	[74]
	Pt-Cu/dendrite	Polyol	Two step process using ascorbic acid	0.5[a]	0.1 M $HClO_4$ + 1.0 M CH_3OH	[36]
	Pt-Pd/cube and tetrahedron	Polyol	Presence of Br^-/I^- ions, $Na_2C_2O_4$, and formaldehyde	1.49[a] (cube) 1.12[a] (tetrahedron)	0.1 M $HClO_4$ + 1.0 M CH_3OH	[75]
	Pt-Pd/octahedron	Polyol	Glycerol/fast reducing rate	~2.2[a]	0.1 M $HClO_4$ + 2.0 M CH_3OH	[41]
	Pt-Cu/hexapod concave with high-index facets	Thermal-decomposition	Concentration of didodecyl dimethyl-ammonium bromide	2.5[a] 1.15[b]	0.5 M H_2SO_4 + 1.0 M CH_3OH	[76]
	Pt-Fe-Co/cube and branched nanocubes	Thermal-decomposition	Etching of acetylacetonate group and presence of N_2 gas	~1.17[b,c]	1.0 M H_2SO_4 + 2.0 M CH_3OH	[77]
	Pt-Co/cube	Thermal-decomposition	Presence of $W(CO)_6$	~1.5[a,c]	0.1 M $HClO_4$ + 1.0 M CH_3OH	[78]
	Pt-Ni/porous nanotube	Electrochemical deposition	ZnO template and deposition time	~1.5[a]	0.5 M H_2SO_4 + 0.5 M CH_3OH	[79]
	Pt-Ru/wires	Electrochemical deposition	AAO template	~13[a]	0.5 M H_2SO_4 + 0.5 M CH_3OH	[80]
EOR	Pt-Bi/nanowires	Polyol	Concentration ratio between Pt and Bi ions	0.65[a,d]	0.1 M $HClO_4$ + 0.125 M CH_3CH_2OH	[32]
	Pt/cube	Polyol	Effect of Fe^{3+} ions	~1.2[a]	0.5 M H_2SO_4 + 2.0 M CH_3CH_2OH	[54]
	Pt/cube	Thermal-decomposition	Presence of PVP	~1.75[a]	0.1 M $HClO_4$ + 2.0 M CH_3CH_2OH	[31]
	Pt/concave with high-index facets	Thermal-decomposition	Presence of formaldehyde	~3.2[b]	0.1 M $HClO_4$ + 0.1 M CH_3CH_2OH	[81]
	Pt-Rh/TPH with high-index facets	Electrochemical deposition	Square-wave potential	4.19[a]	0.1 M $HClO_4$ + 0.1 M CH_3CH_2OH	[82]

[a]Maximum specific area current density (mA cm^{-2}). [b]Maximum specific mass current density (A mg^{-1}). [c]Scan rate is 20 mV s^{-1}. [d]Scan rate is 60 mV s^{-1}.

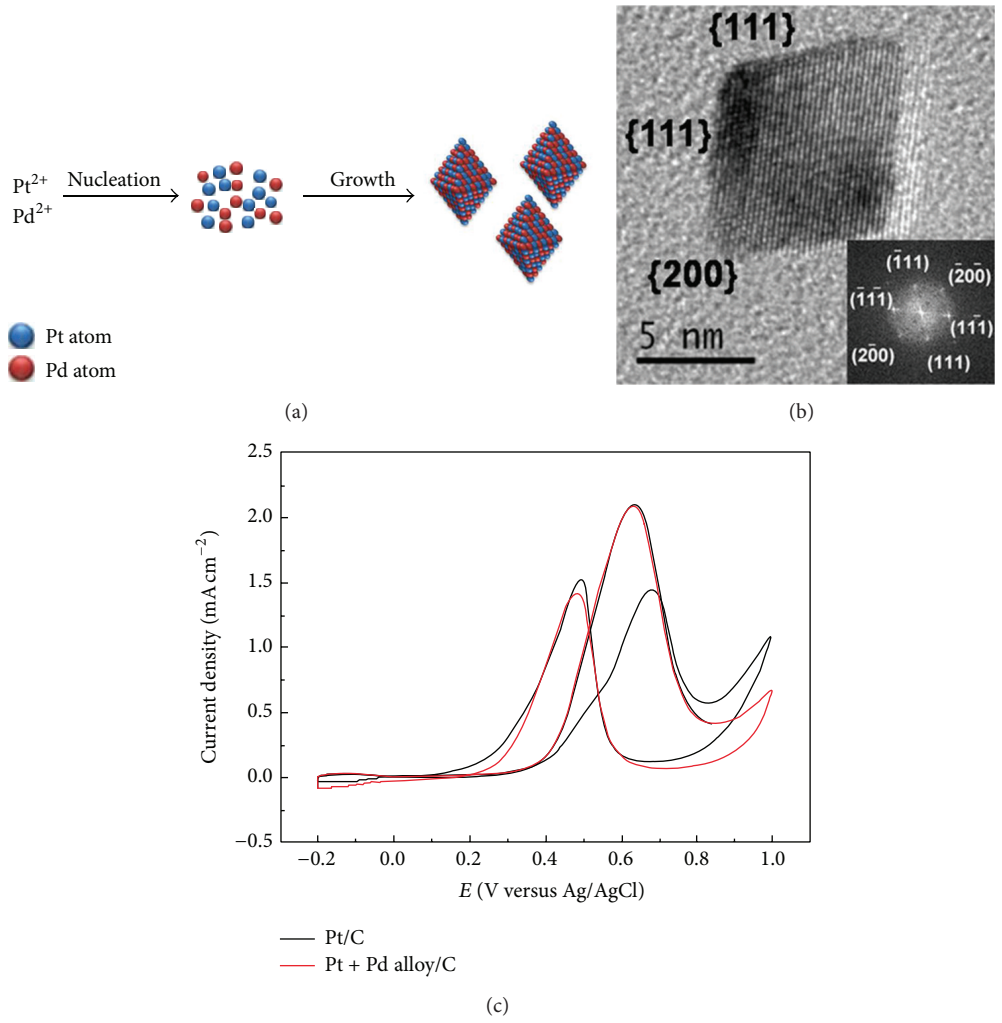

Figure 10: (a) Schematic diagram illustrating the formation of octahedral Pt-Pd alloy nanostructures prepared by glycerol as a reducing agent. (b) HR-TEM images of octahedral Pt-Pd alloy nanostructure. The inset indicates the FFT pattern. (c) CVs of octahedral Pt-Pd alloy nanostructure and commercial Pt electrocatalysts in MOR. Reproduced with permission from [41].

Pt-based alloy catalysts as the most effective catalysts for oxygen electroreduction [102]. In particular, however, there are critical several problems associated with the ORR in low temperature fuel cells, which need to be solved, such as kinetic limitations for oxygen diffusion process and its low long-term stability for oxygen electroreduction. Thus, in order to address these issues, the critical factors, affecting the electrocatalytic properties of Pt-based catalysts, should be considered and identified.

For the enhanced electrochemical activity in the ORR, various Pt-based catalysts with alloy, shape-controlled, and core-shell nanostructures have been reported as shown in Figure 13(a) [103]. Mayrhofer and Arenz showed that nanostructured alloy Pt_3M_1 catalysts can improve the electrocatalytic activity in the ORR due to their modified electronic and surface structures according to the 2nd metallic materials selected in Pt structures in Figure 13(b) [104]. In addition, it has been reported that Pt_xM_y ($x > y$, M = Pd, Ir, Co, Fe, Ni, Y, and Sc) alloy catalysts have greater ORR activity and thermodynamically more stable state in comparison with different elemental compositions of Pt_xM_y ($x \leq y$) or pure Pt catalysts. Moreover, Stamenkovic and coworkers demonstrated that the {111} surface facet of Pt single crystal shows the improved electrochemical activity for ORR compared to the {100} surface facet in an acid electrolyte by utilizing shape-controlled Pt nanostructures [105]. We also developed the synthesis of octahedral Pt_xPd_y nanostructures with various compositions (i.e., Pt_3Pd_1, Pt_1Pd_1, and Pt_1Pd_3), but having dominantly exposed {111} facets, as catalysts for ORRs as indicated in Figure 14(a) [106]. Interestingly, among them, it was found that the octahedral Pt_3Pd_1 nanostructure shows the significantly enhanced electrochemical catalytic activity, such as the increased specific area by 2.35 times and enhanced mass by 1.88 times activity at 0.55 V, and the most stable electrochemical properties in comparison with commercial Pt in Figure 14(b) due to the octahedral shape with dominant {111} facets and favorable elemental composition.

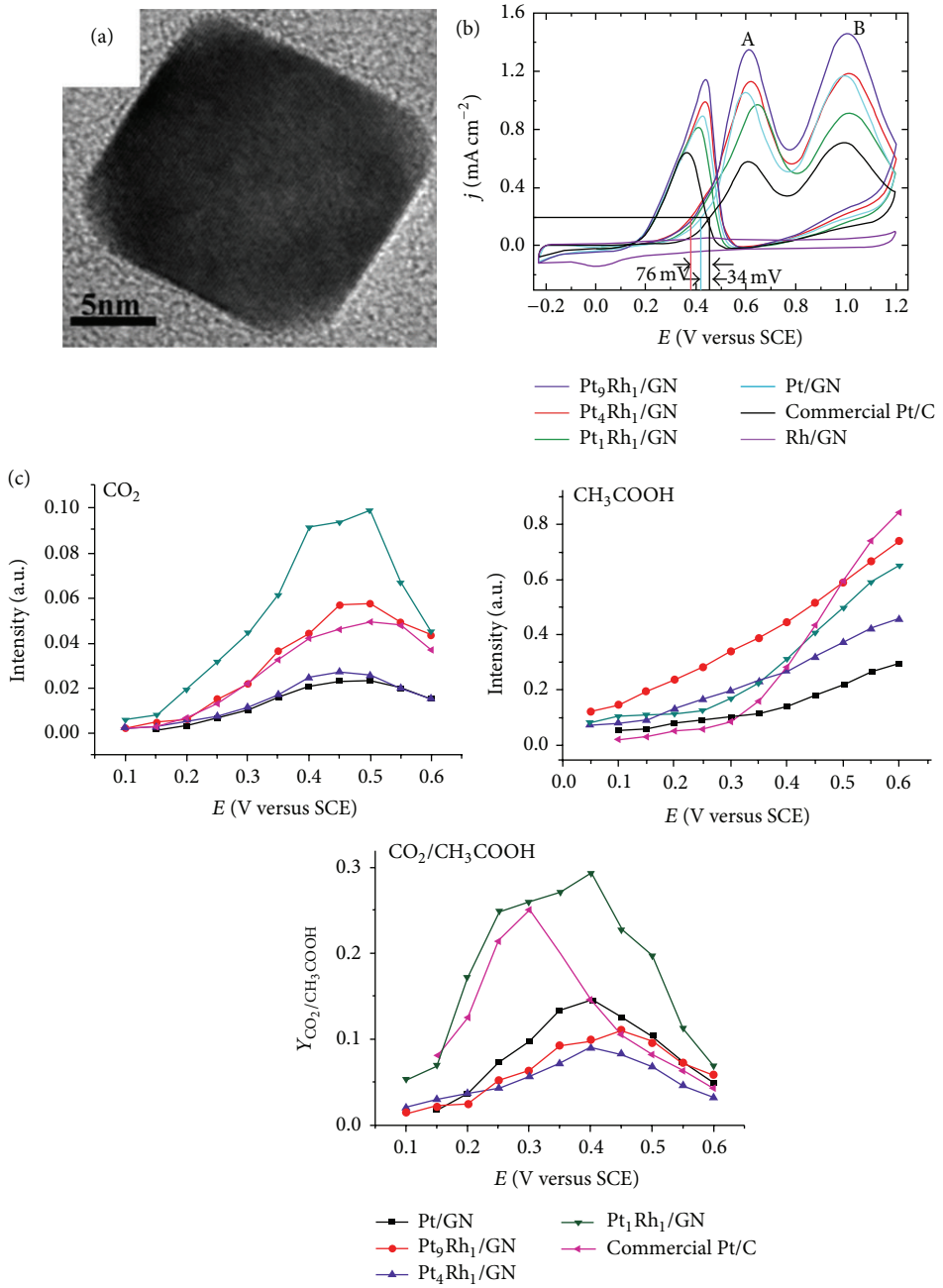

FIGURE 11: (a) HR-TEM image of cubic Pt-Rh nanostructure. (b) CV curves for electrooxidation of formic acid. (c) Integrated band intensities of CO_2 and CH_3COOH in FTIR spectra, and the ratio between integrated intensity with the total oxidation pathway (CO_2) and intensity associated with the partial oxidation pathway (CH_3COOH). Reproduced with permission from [100].

Furthermore, Markovic and coworkers have demonstrated that Pt-Ni alloy nanostructures can be an effective electrocatalyst for the ORR. They showed that Pt_3Ni_1 {111} facet is 10 and 90 times more electrochemically active than Pt {111} facets and commercial Pt in ORRs, respectively, due to their unusual electronic structures for the downshift of d-band center as well as arrangement of surface atoms in the near-surface region in crystal structures [105]. Based on their demonstration of nanostructured Pt-Ni alloy catalysts, many researches have been reported on various nanostructured Pt-Ni alloys. Xia and coworkers demonstrated that octahedral $Pt_{2.5}Ni_1$ nanostructures exhibited highly specific mass activity compared to spherical Pt_3Ni and commercial Pt, because they have the clean catalysts surface and the mostly exposed {111} facets [107]. More recently, in order to maximize surface area, Chen and coworker suggested highly crystalline Pt_3Ni_1 nanoframes with 3D structure [108]. They clearly observed that Pt_3Ni_1 nanoframes significantly enhanced the electrocatalytic mass activity with a world record of 5.7 A mg^{-1}_{Pt} at 0.9 V (versus RHE) in the ORR

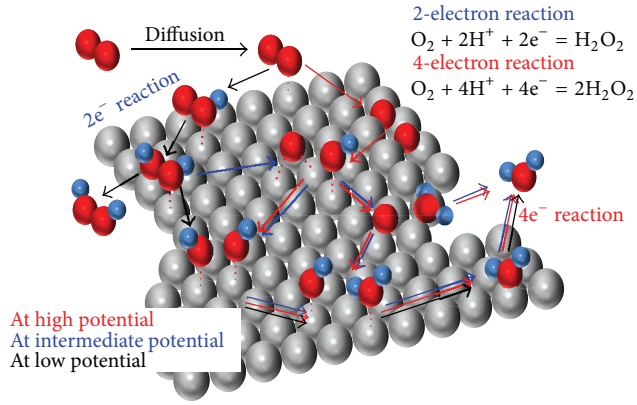

FIGURE 12: (a) Schematic illustration of two electrons and four electrons pathway for oxygen electroreduction reaction in acid electrolyte.

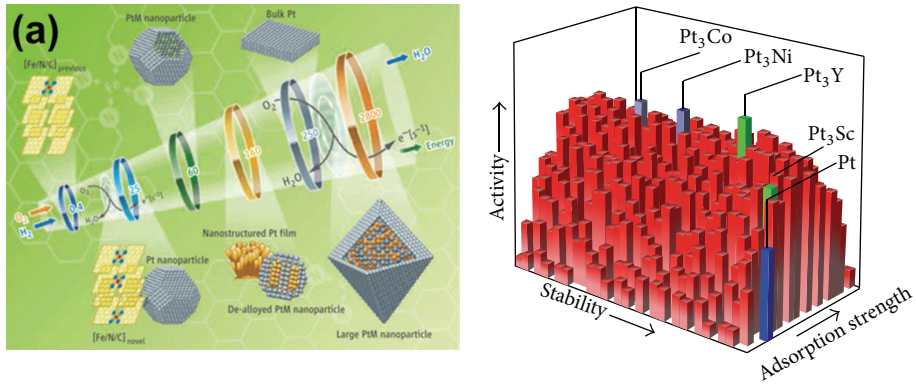

(a) (b)

FIGURE 13: (a) Schematic illustration of research trend of electrocatalysts for ORR. Reproduced with permission from [103]. (b) A three-dimensional "volcano" schematic illustration of Pt-based metal-alloy catalysts in ORR. Reproduced with permission from [104].

due to their high surface-to-volume ratio, 3D surface molecular accessibility for frame structure, and the modulated electronic structure for Pt-Ni alloying phase as shown in Figure 15.

Alternatively, on the basis of expectations that {*hk*1} facets (*h* and/or *k* is greater than one) can improve the electrochemical ORR activities in comparison with the low-index facets, other strategies based on the surface structure modification of Pt nanostructures have been developed to enhance the electrochemical ORR activity. Wang and coworkers demonstrated the synthesis of Pt high concave cubic nanostructures with high-index facets and their utilization for ORR [109]. They showed that the specific mass activity of the Pt concave cubic nanostructures was about 0.71 A mg^{-1}_{Pt} at 0.9 V (versus RHE) in ORR, improved by 2.8 times higher than that of commercial Pt. Additionally, Lim and coworkers also reported the Pd-Pt bimetallic nanodendrites as an ORR electrocatalyst. It was shown that Pd-Pt bimetallic nanodendrites exhibited 2.5 times higher specific mass activity compared to commercial Pt due to their relatively higher surface area resulting from dendritic structures and the exposed {311} facets on branch surface as an active site for ORR [110].

In addition to the development of nanostructured catalysts based on single metal and alloy, many researches have focused on the development of the Pt-based core-shell nanostructures as attractive structures for electrocatalysts in ORR because these structures with designed compositions and morphologies can efficiently reduce the cost of fuel cell manufacturing by significantly reducing the overall amount of Pt required [111–113]. Specially, it would be desirable to reduce the amount of Pt at the cathode because the cathode requires 2~3 times higher Pt loading than required at the anode due to the low kinetic reduction reaction rate in comparison with fuel oxidation reaction. Furthermore, both the exposed surface area and active site density of Pt-based electrocatalysts are very important since the electrochemical reaction in a fuel cell actually occurs on the surface of catalysts. For this reason, many studies have been focused on the control over the shell thickness and composition of Pt-based core-shell nanostructures with inexpensive metal elements as the core and Pt as the shell to enhance specific mass activity in ORR [114]. Wang and coworkers reported that the Cu@Pt core-shell nanoparticles prepared using a galvanic displacement method have approximately 2 times higher specific mass activity than that of commercial Pt/C at 0.85 V (versus NHE) [115]. Additionally, many researches have been reported on a core@Pt-based alloy shell nanostructure in order to increase the catalytic activity and the

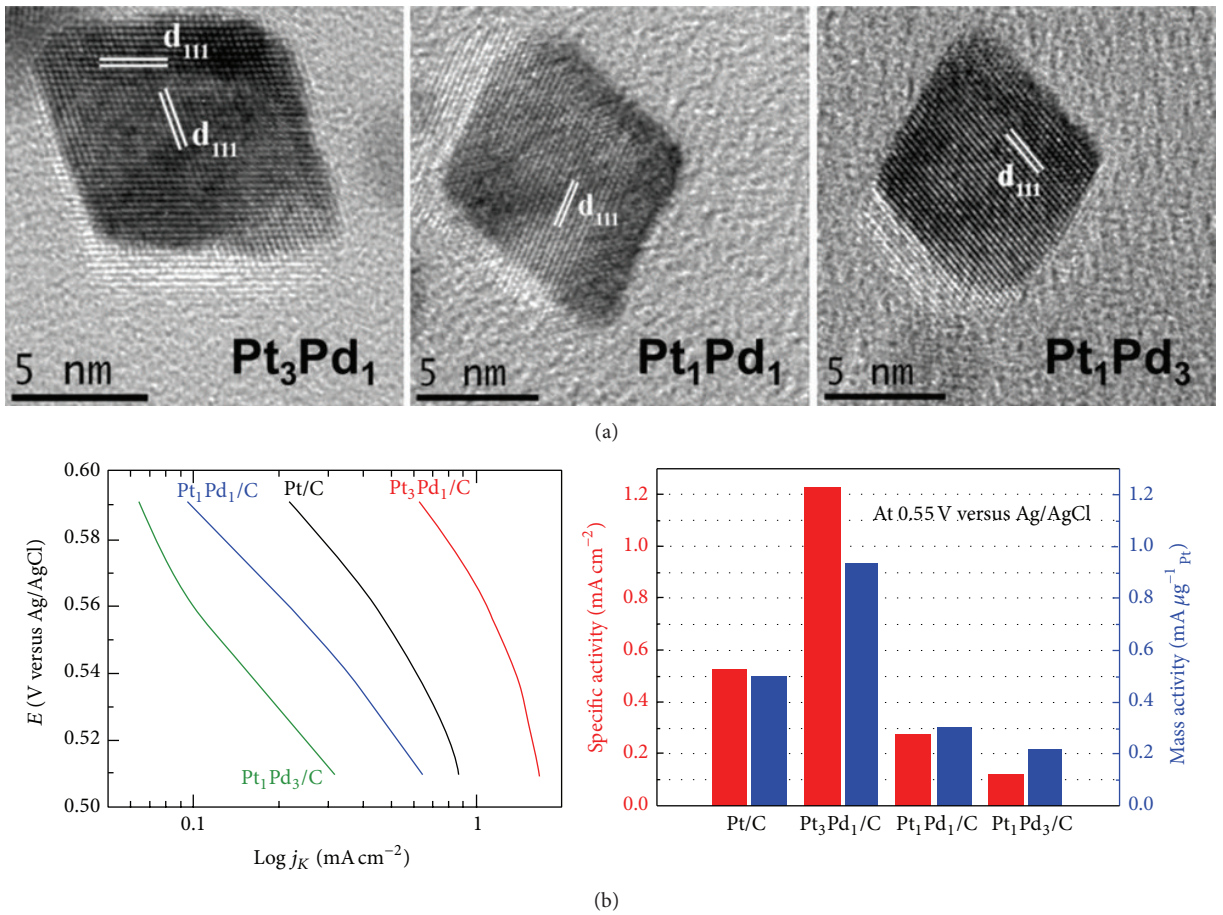

FIGURE 14: (a) TEM images of the octahedral Pt_xPd_y nanostructures. (b) Comparison of specific ORR activities of the octahedral Pt_xPd_y nanostructures and commercial Pt. Reproduced with permission from [106].

TABLE 3: Summary of various Pt-based nanostructures with enhanced electrochemical properties in ORR.

Material/shape	Synthesis method	Experimental factor	I^a, A/mg^{-1}_{Pt}	$E_{1/2}{}^b$, V	Reference
Pt-Pd/core-shell	Polyol	Shell thickness	0.18	0.895	[83]
Pd-Pt/core-shell	Polyol	Seed-mediated growth	~0.2	~0.87	[84]
Pt-Pd/hollow and dendrite	Polyol	Concentration of reductant	~0.76	~0.92	[85]
Pt-Co/truncated octahedron	Thermal-decomposition	Reaction time	0.52	~0.85	[86]
Pt-Ni/truncated octahedron	Thermal-decomposition	Alkane chain length of capping agent	0.53	~0.9	[28]
Pt-Ni/icosahedron	Thermal-decomposition	Presence of CO gas	0.62	0.9	[29]
Pt-Ni/octahedron	Thermal-decomposition	Electrochemical activation	~1.7	~0.92	[30]
Pt-Ni/octahedron	Thermal-decomposition	Reaction time	1.45	~0.92	[87]
Pt-Co/cube	Thermal-decomposition	Composition ratio	0.434	~0.85	[21]
Pt-Fe-Cu/rod	Thermal-decomposition	Electrochemical etching	—	0.557[c]	[33]
Pt-Fe/wire	Thermal-decomposition	Composition ratio	0.84	0.92	[88]
Pt-Fe-Pd/core-shell wire	Thermal-decomposition	Seed-mediated growth	—	~0.55[c]	[89]
Pt/mesoporous	Electrochemical deposition	Silica template	0.12	0.866	[90]
PtCuCoNi/tube	Electrochemical deposition	AAO template	0.19	0.87	[91]
Pt/porous dendrite	Replacement reaction	Replacement reaction	0.21	~0.93	[92]

[a]Specific mass current density at 0.9 V and [b]half-wave potential in ORR polarization curves based on V versus RHE. [c]Half-wave potential (versus Ag/AgCl) in ORR polarization curves.

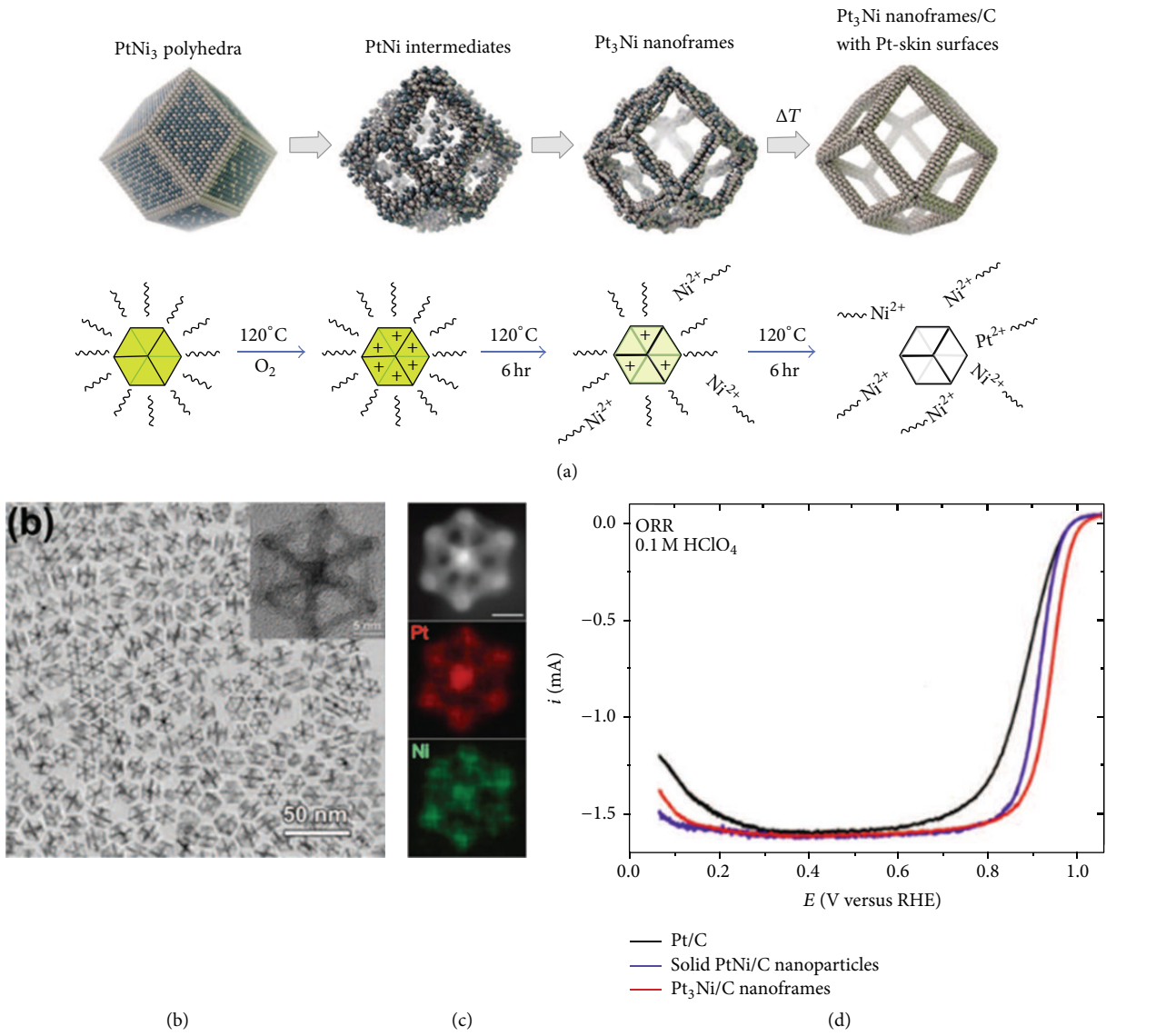

FIGURE 15: (a) Schematic illustration of the chemical and structural evolution process for the Pt_3Ni_1 nanoframes. (b) TEM and (c) EDX elemental mapping images of the Pt_3Ni_1 nanoframes. (d) ORR polarization curves of the Pt_3Ni_1 nanoframes, PtNi/C, and commercial Pt. Reproduced with permission from [108].

specific mass activity [116, 117]. In recent, Choi and coworkers reported that octahedral Pd@Pt-Ni core-shell nanostructures can be synthesized by seeding-mediated and thermal-decomposition methods and that an ORR mass activity (2.5 A mg^{-1}) and a specific activity (2.7 mA cm^{-2}) are 12.5-fold and 14-fold higher than that of commercial Pt/C at 0.9 V (versus RHE), respectively [118]. Mazumder and coworkers also demonstrated the synthesis of the shell thickness-controlled Pd@FePt core-shell nanostructures with 1~3 nm shell thickness for the enhanced electrochemical activity and stability in ORR [119]. They reported that a Pd@FePt nanostructure with 1 nm shell thickness showed 12 times improved specific mass activity compared to commercial Pt due to the thinner alloy FePt shell with higher ORR activity. In order to further provide recent progress in Pt-based electrocatalyst technology, various Pt-based nanostructures with the enhanced catalytic activity and related synthesis approaches are summarized in the Table 3.

4. Conclusions

In summary, we present snapshots of recent research carried out on Pt-based electrocatalysts technology for high performance low-temperature fuel cells, particularly focusing on the recent issues and progress in the development of various synthetic approaches for Pt-based nanostructures with controlled shapes and their electrochemical characteristics of both electrodes. In addition, we describe fundamental aspects of electrochemical reactions and mechanism associated with the shape, dimension, faceted morphology, and composition of nanostructured Pt-based catalyst materials, significantly affecting their electrocatalytic activity. It is expected that this

review will give insights not only into understanding the basic electrochemical mechanism and kinetics of both electrode reactions in fuel cells, but also into developing a genuinely practical electrocatalysts technology for fuel cell commercialization.

Conflict of Interests

The authors declare that there is no conflict of interests regarding the publication of this paper.

Acknowledgments

This work was supported by the International Collaborative Energy Technology R&D Program of the Korea Institute of Energy Technology Evaluation and Planning (KETEP), granted financial resource from the Ministry of Trade, Industry & Energy, Republic of Korea (no. 20138520030800 and 20128510010080).

References

[1] T. R. Ralph, "Proton exchange membrane fuel cells," *Platinum Metals Review*, vol. 41, no. 3, pp. 102–113, 1997.

[2] V. M. Vishnyakov, "Proton exchange membrane fuel cells," *Vacuum*, vol. 80, no. 10, pp. 1053–1065, 2006.

[3] J. Larminie and A. Dicks, *Fuel Cell Systems Explained*, John Wiley & Sons, West Sussex, UK, 2nd edition, 2003.

[4] V. Mehta and J. S. Cooper, "Review and analysis of PEM fuel cell design and manufacturing," *Journal of Power Sources*, vol. 114, no. 1, pp. 32–53, 2003.

[5] H. Liu, C. Song, L. Zhang, J. Zhang, H. Wang, and D. P. Wilkinson, "A review of anode catalysis in the direct methanol fuel cell," *Journal of Power Sources*, vol. 155, no. 2, pp. 95–110, 2006.

[6] X. Cheng, Z. Shi, N. Glass et al., "A review of PEM hydrogen fuel cell contamination: impacts, mechanisms, and mitigation," *Journal of Power Sources*, vol. 165, no. 2, pp. 739–756, 2007.

[7] S. Gottesfeld and J. Pafford, "New approach to the problem of carbon monoxide poisoning in fuel cells operating at low temperatures," *Journal of the Electrochemical Society*, vol. 135, no. 10, pp. 2651–2652, 1988.

[8] P. Waszczuk, A. Wieckowski, P. Zelenay et al., "Adsorption of CO poison on fuel cell nanoparticle electrodes from methanol solutions: a radioactive labeling study," *Journal of Electroanalytical Chemistry*, vol. 511, no. 1-2, pp. 55–64, 2001.

[9] N. M. Markoví and P. N. Ross Jr., "Surface science studies of model fuel cell electrocatalysts," *Surface Science Reports*, vol. 45, no. 4–6, pp. 117–229, 2002.

[10] K. Broka and P. Ekdunge, "Modelling the PEM fuel cell cathode," *Journal of Applied Electrochemistry*, vol. 27, no. 3, pp. 281–289, 1997.

[11] Y.-W. Lee, S.-E. Oh, and K.-W. Park, "Highly active Pt-Pd alloy catalyst for oxygen reduction reaction in buffer solution," *Electrochemistry Communications*, vol. 13, no. 12, pp. 1300–1303, 2011.

[12] S. Guo, S. Dong, and E. Wang, "Three-dimensional Pt-on-Pd bimetallic nanodendrites supported on graphene nanosheet: facile synthesis and used as an advanced nanoelectrocatalyst for methanol oxidation," *ACS Nano*, vol. 4, no. 1, pp. 547–555, 2010.

[13] F. Nosheen, Z. Zhang, G. Xiang et al., "Three-dimensional hierarchical Pt–Cu superstructures," *Nano Research*, vol. 8, no. 3, pp. 832–838, 2015.

[14] D. Zhang, W. Gao, X. Xia, and H. Chen, "Three-dimensional ordered macroporous platinum-based electrode for methanol oxidation," *Chinese Science Bulletin*, vol. 51, no. 1, pp. 19–24, 2006.

[15] D.-H. Kwak, Y.-W. Lee, S.-B. Han et al., "Ultrasmall PtSn alloy catalyst for ethanol electro-oxidation reaction," *Journal of Power Sources*, vol. 275, pp. 557–562, 2015.

[16] K.-W. Park, Y.-W. Lee, and Y.-E. Sung, "Nanostructure catalysts prepared by multi-sputtering deposition process for enhanced methanol electrooxidation reaction," *Applied Catalysis B: Environmental*, vol. 132-133, pp. 237–244, 2013.

[17] R. Loukrakpam, J. Luo, T. He et al., "Nanoengineered PtCo and PtNi catalysts for oxygen reduction reaction: an assessment of the structural and electrocatalytic properties," *Journal of Physical Chemistry C*, vol. 115, no. 5, pp. 1682–1694, 2011.

[18] T.-Y. Chen, T.-J. M. Luo, Y.-W. Yang et al., "Core dominated surface activity of core-shell nanocatalysts on methanol electrooxidation," *The Journal of Physical Chemistry C*, vol. 116, no. 32, pp. 16969–16978, 2012.

[19] M. Shao, B. H. Smith, S. Guerrero et al., "Core-shell catalysts consisting of nanoporous cores for oxygen reduction reaction," *Physical Chemistry Chemical Physics*, vol. 15, no. 36, pp. 15078–15090, 2013.

[20] S.-I. Choi, S. Xie, M. Shao et al., "Controlling the size and composition of nanosized Pt-Ni octahedra to optimize their catalytic activities toward the oxygen reduction reaction," *ChemSusChem*, vol. 7, no. 5, pp. 1476–1483, 2014.

[21] S.-I. Choi, S.-U. Lee, W. Y. Kim et al., "Composition-controlled PtCo alloy nanocubes with tuned electrocatalytic activity for oxygen reduction," *ACS Applied Materials & Interfaces*, vol. 4, no. 11, pp. 6228–6234, 2012.

[22] J. H. Kim, S. M. Choi, S. H. Nam, M. H. Seo, S. H. Choi, and W. B. Kim, "Influence of Sn content on PtSn/C catalysts for electrooxidation of C_1-C_3 alcohols: synthesis, characterization, and electrocatalytic activity," *Applied Catalysis B: Environmental*, vol. 82, no. 1-2, pp. 89–102, 2008.

[23] G. Zhou, M. Lu, and Z. Yang, "Aqueous synthesis of copper nanocubes and bimetallic copper/palladium core-shell nanostructures," *Langmuir*, vol. 22, no. 13, pp. 5900–5903, 2006.

[24] Y.-W. Lee, S.-B. Han, and K.-W. Park, "Electrochemical properties of Pd nanostructures in alkaline solution," *Electrochemistry Communications*, vol. 11, no. 10, pp. 1968–1971, 2009.

[25] H. Lee, S. E. Habas, S. Kweskin, D. Butcher, G. A. Somorjai, and P. Yang, "Morphological control of catalytically active platinum nanocrystals," *Angewandte Chemie—International Edition*, vol. 45, no. 46, pp. 7824–7828, 2006.

[26] S.-I. Choi, R. Choi, S. W. Han, and J. T. Park, "Synthesis and characterization of Pt_9Co nanocubes with high activity for oxygen reduction," *Chemical Communications*, vol. 46, no. 27, pp. 4950–4952, 2010.

[27] S. Eustis, H.-Y. Hsu, and M. A. El-Sayed, "Gold nanoparticle formation from photochemical reduction of Au^{3+} by continuous excitation in colloidal solutions. A proposed molecular mechanism," *The Journal of Physical Chemistry B*, vol. 109, no. 11, pp. 4811–4815, 2005.

[28] J. Wu, J. Zhang, Z. Peng, S. Yang, F. T. Wagner, and H. Yang, "Truncated octahedral Pt_3Ni oxygen reduction reaction electrocatalysts," *Journal of the American Chemical Society*, vol. 132, no. 14, pp. 4984–4985, 2010.

[29] J. Wu, L. Qi, H. You, A. Gross, J. Li, and H. Yang, "Icosahedral platinum alloy nanocrystals with enhanced electrocatalytic activities," *Journal of the American Chemical Society*, vol. 134, no. 29, pp. 11880–11883, 2012.

[30] C. Cui, L. Gan, M. Heggen, S. Rudi, and P. Strasser, "Compositional segregation in shaped Pt alloy nanoparticles and their structural behaviour during electrocatalysis," *Nature Materials*, vol. 12, no. 8, pp. 765–771, 2013.

[31] Y.-W. Lee, S.-B. Han, D.-Y. Kim, and K.-W. Park, "Monodispersed platinum nanocubes for enhanced electrocatalytic properties in alcohol electrooxidation," *Chemical Communications*, vol. 47, no. 22, pp. 6296–6298, 2011.

[32] W. Du, D. Su, Q. Wang, A. I. Frenkel, and X. Teng, "Promotional effects of bismuth on the formation of platinum-bismuth nanowires network and the electrocatalytic activity toward ethanol oxidation," *Crystal Growth & Design*, vol. 11, no. 2, pp. 594–599, 2011.

[33] H. Zhu, S. Zhang, S. Guo, D. Su, and S. Sun, "Synthetic control of FePtM nanorods (M = Cu, Ni) to enhance the oxygen reduction reaction," *Journal of the American Chemical Society*, vol. 135, no. 19, pp. 7130–7133, 2013.

[34] X. Huang, S. Tang, X. Mu et al., "Freestanding palladium nanosheets with plasmonic and catalytic properties," *Nature Nanotechnology*, vol. 6, no. 1, pp. 28–32, 2011.

[35] Y. Xiong, I. Washio, J. Chen, H. Cai, Z.-Y. Li, and Y. Xia, "Poly (vinyl pyrrolidone): a dual functional reductant and stabilizer for the facile synthesis of noble metal nanoplates in aqueous solutions," *Langmuir*, vol. 22, no. 20, pp. 8563–8570, 2006.

[36] E. Taylor, S. Chen, J. Tao, L. Wu, Y. Zhu, and J. Chen, "Synthesis of Pt-Cu nanodendrites through controlled reduction kinetics for enhanced methanol electro-oxidation," *ChemSusChem*, vol. 6, no. 10, pp. 1863–1867, 2013.

[37] X. T. Du, Y. Yang, J. Liu et al., "Surfactant-free and template-free electrochemical approach to prepare well-dispersed Pt nanosheets and their high electrocatalytic activities for ammonia oxidation," *Electrochimica Acta*, vol. 111, pp. 562–566, 2013.

[38] F. Fievet, J. P. Lagier, B. Blin, B. Beaudoin, and M. Figlarz, "Homogeneous and heterogeneous nucleations in the polyol process for the preparation of micron and submicron size metal particles," *Solid State Ionics*, vol. 32-33, no. 1, pp. 198–205, 1989.

[39] H. Zhang, M. Jin, Y. Xiong, B. Lim, and Y. Xia, "Shape-controlled synthesis of Pd nanocrystals and their catalytic applications," *Accounts of Chemical Research*, vol. 46, no. 8, pp. 1783–1794, 2013.

[40] B. Lim, M. Jiang, J. Tao, P. H. C. Camargo, Y. Zhu, and Y. Xia, "Shape-controlled synthesis of Pd nanocrystals in aqueous solutions," *Advanced Functional Materials*, vol. 19, no. 2, pp. 189–200, 2009.

[41] Y.-W. Lee, A.-R. Ko, S.-B. Han, H.-S. Kim, and K.-W. Park, "Synthesis of octahedral Pt-Pd alloy nanoparticles for improved catalytic activity and stability in methanol electrooxidation," *Physical Chemistry Chemical Physics*, vol. 13, no. 13, pp. 5569–5572, 2011.

[42] L. Vitos, A. V. Ruban, H. L. Skriver, and J. Kollár, "The surface energy of metals," *Surface Science*, vol. 411, no. 1-2, pp. 186–202, 1998.

[43] L. J. Giovanetti, J. M. Ramallo-Lõpez, M. Foxe et al., "Shape changes of Pt nanoparticles induced by deposition on mesoporous silica," *Small*, vol. 8, no. 3, pp. 468–473, 2012.

[44] H.-L. Wu, C.-H. Kuo, and M. H. Huang, "Seed-mediated synthesis of gold nanocrystals with systematic shape evolution from cubic to trisoctahedral and rhombic dodecahedral structures," *Langmuir*, vol. 26, no. 14, pp. 12307–12313, 2010.

[45] S. Yang, F. Hong, L. Wang et al., "Ultrathin pt-based alloy nanowire networks: synthesized by CTAB assistant two-phase water-chloroform micelles," *The Journal of Physical Chemistry C*, vol. 114, no. 1, pp. 203–207, 2010.

[46] C. Kim and H. Lee, "Change in the catalytic reactivity of Pt nanocubes in the presence of different surface-capping agents," *Catalysis Communications*, vol. 10, no. 9, pp. 1305–1309, 2009.

[47] J. Zeng, Y. Zheng, M. Rycenga et al., "Controlling the shapes of silver nanocrystals with different capping agents," *Journal of the American Chemical Society*, vol. 132, no. 25, pp. 8552–8553, 2010.

[48] X. Xia, J. Zeng, L. K. Oetjen, Q. Li, and Y. Xia, "Quantitative analysis of the role played by poly(vinylpyrrolidone) in seed-mediated growth of Ag nanocrystals," *Journal of the American Chemical Society*, vol. 134, no. 3, pp. 1793–1801, 2012.

[49] V. Mazumder and S. Sun, "Oleylamine-mediated synthesis of Pd nanoparticles for catalytic formic acid oxidation," *Journal of the American Chemical Society*, vol. 131, no. 13, pp. 4588–4589, 2009.

[50] N. Naresh, F. G. S. Wasim, B. P. Ladewig, and M. Neergat, "Removal of surfactant and capping agent from Pd nanocubes (Pd-NCs) using tert-butylamine: its effect on electrochemical characteristics," *Journal of Materials Chemistry A*, vol. 1, no. 30, pp. 8553–8559, 2013.

[51] C. Aliaga, J. Y. Park, Y. Yamada et al., "Sum frequency generation and catalytic reaction studies of the removal of organic capping agents from Pt nanoparticles by UV-Ozone treatment," *Journal of Physical Chemistry C*, vol. 113, no. 15, pp. 6150–6155, 2009.

[52] C. Susut, T. D. Nguyen, G. B. Chapman, and Y. Tong, "Shape and size stability of Pt nanoparticles for MeOH electro-oxidation," *Electrochimica Acta*, vol. 53, no. 21, pp. 6135–6142, 2008.

[53] H. Song, F. Kim, S. Connor, G. A. Somorjai, and P. Yang, "Pt nanocrystals: shape control and Langmuir-Blodgett monolayer formation," *The Journal of Physical Chemistry B*, vol. 109, no. 1, pp. 188–193, 2005.

[54] S.-B. Han, Y.-J. Song, J.-M. Lee, J.-Y. Kim, and K.-W. Park, "Platinum nanocube catalysts for methanol and ethanol electrooxidation," *Electrochemistry Communications*, vol. 10, no. 7, pp. 1044–1047, 2008.

[55] T. Herricks, J. Chen, and Y. Xia, "Polyol synthesis of platinum nanoparticles: control of morphology with sodium nitrate," *Nano Letters*, vol. 4, no. 12, pp. 2367–2371, 2004.

[56] C. Wang, H. Daimon, T. Onodera, T. Koda, and S. Sun, "A general approach to the size- and shape-controlled synthesis of platinum nanoparticles and their catalytic reduction of oxygen," *Angewandte Chemie*, vol. 47, no. 19, pp. 3588–3591, 2008.

[57] Y. Yu, W. Yang, X. Sun et al., "Monodisperse MPt (M = Fe, Co, Ni, Cu, Zn) nanoparticles prepared from a facile oleylamine reduction of metal salts," *Nano Letters*, vol. 14, no. 5, pp. 2778–2782, 2014.

[58] M. A. Mahmoud, B. Snyder, and M. A. El-Sayed, "Polystyrene microspheres: inactive supporting material for recycling and recovering colloidal nanocatalysts in solution," *Journal of Physical Chemistry Letters*, vol. 1, no. 1, pp. 28–31, 2010.

[59] Q. Wang, B. Geng, and B. Tao, "A facile room temperature chemical route to Pt nanocube/carbon nanotube heterostructures with enhanced electrocatalysis," *Journal of Power Sources*, vol. 196, no. 1, pp. 191–195, 2011.

[60] J. Zhang and J. Fang, "A general strategy for preparation of Pt 3d-transition metal (Co, Fe, Ni) nanocubes," *Journal of the American Chemical Society*, vol. 131, no. 51, pp. 18543–18547, 2009.

[61] B. Wu, N. Zheng, and G. Fu, "Small molecules control the formation of Pt nanocrystals: a key role of carbon monoxide in the synthesis of Pt nanocubes," *Chemical Communications*, vol. 47, no. 3, pp. 1039–1041, 2011.

[62] N. Tian, Z.-Y. Zhou, S.-G. Sun, Y. Ding, and L. W. Zhong, "Synthesis of tetrahexahedral platinum nanocrystals with high-index facets and high electro-oxidation activity," *Science*, vol. 316, no. 5825, pp. 732–735, 2007.

[63] J. B. Raoof, R. Ojani, and S. R. Hosseini, "Electrochemical synthesis of a novel platinum nanostructure on a glassy carbon electrode, and its application to the electrooxidation of methanol," *Microchimica Acta*, vol. 180, no. 9-10, pp. 879–886, 2013.

[64] H. Gu, Y. Yang, J. Tian, and G. Shi, "Photochemical synthesis of noble metal (Ag, Pd, Au, Pt) on graphene/ZnO multihybrid nanoarchitectures as electrocatalysis for H_2O_2 reduction," *ACS Applied Materials & Interfaces*, vol. 5, no. 14, pp. 6762–6768, 2013.

[65] S. F. Chen, J. P. Li, K. Qian et al., "Large scale photochemical synthesis of M@TiO_2 nanocomposites (M = Ag, Pd, Au, Pt) and their optical properties, CO oxidation performance, and antibacterial effect," *Nano Research*, vol. 3, no. 4, pp. 244–255, 2010.

[66] R. Ojani, J.-B. Raoof, and S. Safshekan, "Photoinduced deposition of palladium nanoparticles on TiO_2 nanotube electrode and investigation of its capability for formaldehyde oxidation," *Electrochimica Acta*, vol. 138, pp. 468–475, 2014.

[67] X. Huang, X. Qi, Y. Huang et al., "Photochemically controlled synthesis of anisotropic Au nanostructures: platelet-like Au nanorods and six-star Au nanoparticles," *ACS Nano*, vol. 4, no. 10, pp. 6196–6202, 2010.

[68] S. Chen, H. Su, Y. Wang, W. Wu, and J. Zeng, "Size-controlled synthesis of platinum-copper hierarchical trigonal bipyramid nanoframes," *Angewandte Chemie International Edition*, vol. 137, no. 1, pp. 110–115, 2014.

[69] J. Zhang, H. Yang, K. Yang et al., "Monodisperse Pt_3Fe nanocubes: synthesis, characterization, self-assembly, and electrocatalytic activity," *Advanced Functional Materials*, vol. 20, no. 21, pp. 3727–3733, 2010.

[70] M. Subhramannia, K. Ramaiyan, and V. K. Pillai, "Comparative study of the shape-dependent electrocatalytic activity of platinum multipods, discs, and hexagons: applications for fuel cells," *Langmuir*, vol. 24, no. 7, pp. 3576–3583, 2008.

[71] Y. Kim, H. J. Kim, Y. S. Kim, S. M. Choi, M. H. Seo, and W. B. Kim, "Shape- and composition-sensitive activity of Pt and PtAu catalysts for formic acid electrooxidation," *Journal of Physical Chemistry C*, vol. 116, no. 34, pp. 18093–18100, 2012.

[72] Y. Li, Y. Jiang, M. Chen et al., "Electrochemically shape-controlled synthesis of trapezohedral platinum nanocrystals with high electrocatalytic activity," *Chemical Communications*, vol. 48, no. 76, pp. 9531–9533, 2012.

[73] G. Fu, R. Ma, X. Gao et al., "Hydrothermal synthesis of Pt-Ag alloy nano-octahedra and their enhanced electrocatalytic activity for the methanol oxidation reaction," *Nanoscale*, vol. 6, no. 21, pp. 12310–12314, 2014.

[74] X. Huang, Y. Chen, E. Zhu, Y. Xu, X. Duan, and Y. Huang, "Monodisperse Cu@PtCu nanocrystals and their conversion into hollow-PtCu nanostructures for methanol oxidation," *Journal of Materials Chemistry A*, vol. 1, no. 46, pp. 14449–14454, 2013.

[75] A.-X. Yin, X.-Q. Min, Y.-W. Zhang, and C.-H. Yan, "Shape-selective synthesis and facet-dependent enhanced electrocatalytic activity and durability of monodisperse Sub-10 nm Pt-Pd tetrahedrons and cubes," *Journal of the American Chemical Society*, vol. 133, no. 11, pp. 3816–3819, 2011.

[76] X. Liu, W. Wang, H. Li et al., "One-pot protocol for bimetallic Pt/Cu hexapod concave nanocrystals with enhanced electrocatalytic activity," *Scientific Reports*, vol. 3, article 1404, 2013.

[77] S. S. Kim, C. Kim, and H. Lee, "Shape- and composition-controlled Pt-Fe-Co nanoparticles for electrocatalytic methanol oxidation," *Topics in Catalysis*, vol. 53, no. 7&10, pp. 686–693, 2010.

[78] H. Yang, J. Zhang, K. Sun, S. Zou, and J. Fang, "Enhancing by weakening: electrooxidation of methanol on Pt_3Co and Pt nanocubes," *Angewandte Chemie International Edition*, vol. 49, no. 38, pp. 6848–6851, 2010.

[79] L.-X. Ding, G.-R. Li, Z.-L. Wang, Z.-Q. Liu, H. Liu, and Y.-X. Tong, "Porous Ni@Pt core-shell nanotube array electrocatalyst with high activity and stability for methanol oxidation," *Chemistry—A European Journal*, vol. 18, no. 27, pp. 8386–8391, 2012.

[80] G.-Y. Zhao, C.-L. Xu, D.-J. Guo, H. Li, and H.-L. Li, "Template preparation of Pt-Ru and Pt nanowire array electrodes on a Ti/Si substrate for methanol electro-oxidation," *Journal of Power Sources*, vol. 162, no. 1, pp. 492–496, 2006.

[81] L. Zhang, D. Chen, Z. Jiang et al., "Facile syntheses and enhanced electrocatalytic activities of Pt nanocrystals with {*hkk*} high-index surfaces," *Nano Research*, vol. 5, no. 3, pp. 181–189, 2012.

[82] N. Tian, J. Xiao, Z.-Y. Zhou et al., "Pt-group bimetallic nanocrystals with high-index facets as high performance electrocatalysts," *Faraday Discussions*, vol. 162, pp. 77–89, 2013.

[83] R. Choi, S.-I. Choi, C. H. Choi et al., "Designed synthesis of well-defined Pd@Pt core-shell nanoparticles with controlled shell thickness as efficient oxygen reduction electrocatalysts," *Chemistry: A European Journal*, vol. 19, no. 25, pp. 8190–8198, 2013.

[84] L. Liu, G. Samjeske, S.-I. Nagamatsu et al., "Enhanced oxygen reduction reaction activity and characterization of Pt-Pd/C bimetallic fuel cell catalysts with pt-enriched surfaces in acid media," *Journal of Physical Chemistry C*, vol. 116, no. 44, pp. 23453–23464, 2012.

[85] J. W. Hong, S. W. Kang, B.-S. Choi, D. Kim, S. B. Lee, and S. W. Han, "Controlled synthesis of Pd-Pt alloy hollow nanostructures with enhanced catalytic activities for oxygen reduction," *ACS Nano*, vol. 6, no. 3, pp. 2410–2419, 2012.

[86] S.-I. Choi, R. Choi, S. W. Han, and J. T. Park, "Shape-controlled synthesis of Pt_3Co nanocrystals with high electrocatalytic activity toward oxygen reduction," *Chemistry—A European Journal*, vol. 17, no. 44, pp. 12280–12284, 2011.

[87] C. Cui, L. Gan, H.-H. Li, S.-H. Yu, M. Heggen, and P. Strasser, "Octahedral PtNi nanoparticle catalysts: exceptional oxygen reduction activity by tuning the alloy particle surface composition," *Nano Letters*, vol. 12, no. 11, pp. 5885–5889, 2012.

[88] S. Guo, D. Li, H. Zhu et al., "FePt and CoPt nanowires as efficient catalysts for the oxygen reduction reaction," *Angewandte Chemie—International Edition*, vol. 52, no. 12, pp. 3465–3468, 2013.

[89] S. Guo, S. Zhang, D. Su, and S. Sun, "Seed-mediated synthesis of core/shell FePtM/FePt (M = Pd, Au) nanowires and their electrocatalysis for oxygen reduction reaction," *Journal of the*

American Chemical Society, vol. 135, no. 37, pp. 13879–13884, 2013.

[90] J. Kibsgaard, Y. Gorlin, Z. Chen, and T. F. Jaramillo, "Meso-structured platinum thin films: active and stable electrocatalysts for the oxygen reduction reaction," *Journal of the American Chemical Society*, vol. 134, no. 18, pp. 7758–7765, 2012.

[91] L. Liu and E. Pippel, "Low-platinum-content quaternary PtCu-CoNi nanotubes with markedly enhanced oxygen reduction activity," *Angewandte Chemie International Edition*, vol. 50, no. 12, pp. 2729–2733, 2011.

[92] G. Zhang, S. Sun, M. Cai, Y. Zhang, R. Li, and X. Sun, "Porous dendritic platinum nanotubes with extremely high activity and stability for oxygen reduction reaction," *Scientific Reports*, vol. 3, article 1526, 2013.

[93] H. A. Gasteiger, N. Markovic, P. N. Ross Jr., and E. J. Cairns, "Carbon monoxide electrooxidation on well-characterized platinum-ruthenium alloys," *The Journal of Physical Chemistry*, vol. 98, no. 2, pp. 617–625, 1994.

[94] M. Osawa, K.-I. Komatsu, G. Samjeské et al., "The role of bridge-bonded adsorbed formate in the electrocatalytic oxidation of formic acid on platinum," *Angewandte Chemie International Edition*, vol. 50, no. 5, pp. 1159–1163, 2011.

[95] Y.-W. Lee, B.-Y. Kim, K.-H. Lee, W.-J. Song, G. Cao, and K.-W. Park, "Synthesis of monodispersed Pt-Ni alloy nanodendrites and their electrochemical properties," *International Journal of Electrochemical Science*, vol. 8, no. 2, pp. 2305–2312, 2013.

[96] X. Huang, Z. Zhao, J. Fan, Y. Tan, and N. Zheng, "Amine-assisted synthesis of concave polyhedral platinum nanocrystals having {411} high-index facets," *Journal of the American Chemical Society*, vol. 133, no. 13, pp. 4718–4721, 2011.

[97] J. Solla-Gullón, F. J. Vidal-Iglesias, A. López-Cudero, E. Garnier, J. M. Feliu, and A. Aldaz, "Shape-dependent electrocatalysis: methanol and formic acid electrooxidation on preferentially oriented Pt nanoparticles," *Physical Chemistry Chemical Physics*, vol. 10, no. 25, pp. 3689–3698, 2008.

[98] Y. Li and Y. Huang, "Low-temperature, seed-mediated synthesis of monodispersed hyperbranched PtRu nanoparticles and their electrocatalytic activity in methanol oxidation," *Journal of Materials Chemistry*, vol. 22, no. 25, pp. 12461–12464, 2012.

[99] Y. Qi, T. Bian, S.-I. Choi et al., "Kinetically controlled synthesis of Pt-Cu alloy concave nanocubes with high-index facets for methanol electro-oxidation," *Chemical Communications*, vol. 50, no. 5, pp. 560–562, 2014.

[100] L. Rao, Y.-X. Jiang, B.-W. Zhang, Y.-R. Cai, and S.-G. Sun, "High activity of cubic PtRh alloys supported on graphene towards ethanol electrooxidation," *Physical Chemistry Chemical Physics*, vol. 16, no. 27, pp. 13662–13671, 2014.

[101] Q. Yuan, Z. Zhou, J. Zhuang, and X. Wang, "Tunable aqueous phase synthesis and shape-dependent electrochemical properties of rhodium nanostructures," *Inorganic Chemistry*, vol. 49, no. 12, pp. 5515–5521, 2010.

[102] J. A. Keith and T. Jacob, "Theoretical studies of potential-dependent and competing mechanisms of the electrocatalytic oxygen reduction reaction on Pt(111)," *Angewandte Chemie*, vol. 49, no. 49, pp. 9521–9525, 2010.

[103] H. A. Gasteiger and N. M. Markovic, "Just a dream—or future reality?" *Science*, vol. 324, no. 5923, pp. 48–49, 2009.

[104] K. J. J. Mayrhofer and M. Arenz, "Fuel cells: log on for new catalysts," *Nature Chemistry*, vol. 1, no. 7, pp. 518–519, 2009.

[105] V. R. Stamenkovic, B. Fowler, B. S. Mun et al., "Improved oxygen reduction activity on Pt3Ni(111) via increased surface site availability," *Science*, vol. 315, no. 5811, pp. 493–497, 2007.

[106] Y.-W. Lee, A.-R. Ko, D.-Y. Kim, S.-B. Han, and K.-W. Park, "Octahedral Pt-Pd alloy catalysts with enhanced oxygen reduction activity and stability in proton exchange membrane fuel cells," *RSC Advances*, vol. 2, no. 3, pp. 1119–1125, 2012.

[107] S.-I. Choi, S. Xie, M. Shao et al., "Synthesis and characterization of 9 nm Pt-Ni octahedra with a record high activity of 3.3 A/mg_{Pt} for the oxygen reduction reaction," *Nano Letters*, vol. 13, no. 7, pp. 3420–3425, 2013.

[108] C. Chen, Y. Kang, Z. Huo et al., "Highly crystalline multimetallic nanoframes with three-dimensional electrocatalytic surfaces," *Science*, vol. 343, no. 6177, pp. 1339–1343, 2014.

[109] C. Wang, L. Ma, L. Liao et al., "A unique platinum-graphene hybrid structure for high activity and durability in oxygen reduction reaction," *Scientific Reports*, vol. 3, article 2580, 2013.

[110] B. Lim, M. Jiang, P. H. C. Camargo et al., "Pd-Pt bimetallic nanodendrites with high activity for oxygen reduction," *Science*, vol. 324, no. 5932, pp. 1302–1305, 2009.

[111] M. Neergat and R. Rahul, "Unsupported Cu-Pt core-shell nanoparticles: oxygen reduction reaction (ORR) catalyst with better activity and reduced precious metal content," *Journal of the Electrochemical Society*, vol. 159, no. 7, pp. F234–F241, 2012.

[112] K. Gong, D. Su, and R. R. Adzic, "Platinum-monolayer shell on $AuNi_{0.5}Fe$ nanoparticle core electrocatalyst with high activity and stability for the oxygen reduction reaction," *Journal of the American Chemical Society*, vol. 132, no. 41, pp. 14364–14366, 2010.

[113] D. Wang, H. L. Xin, R. Hovden et al., "Structurally ordered intermetallic platinum-cobalt core-shell nanoparticles with enhanced activity and stability as oxygen reduction electrocatalysts," *Nature Materials*, vol. 12, no. 1, pp. 81–87, 2013.

[114] S. Zhang, Y. Hao, D. Su et al., "Monodisperse core/shell Ni/FePt nanoparticles and their conversion to Ni/Pt to catalyze oxygen reduction," *Journal of the American Chemical Society*, vol. 136, no. 45, pp. 15921–15924, 2014.

[115] G. Wang, H. Wu, D. Wexler, H. Liu, and O. Savadogo, "Ni@Pt core-shell nanoparticles with enhanced catalytic activity for oxygen reduction reaction," *Journal of Alloys and Compounds*, vol. 503, no. 1, pp. L1–L4, 2010.

[116] A. Sarkar and A. Manthiram, "Synthesis of Pt@Cu Core-shell nanoparticles by galvanic displacement of Cu by Pt^{4+} ions and their application as electrocatalysts for oxygen reduction reaction in fuel cells," *Journal of Physical Chemistry C*, vol. 114, no. 10, pp. 4725–4732, 2010.

[117] C. Wang, D. van der Vliet, K. L. More et al., "Multimetallic Au/FePt3 nanoparticles as highly durable electrocatalyst," *Nano Letters*, vol. 11, no. 3, pp. 919–926, 2011.

[118] S.-I. Choi, M. Shao, N. Lu et al., "Synthesis and characterization of Pd@Pt-Ni core-shell octahedra with high activity toward oxygen reduction," *ACS Nano*, vol. 8, no. 10, pp. 10363–10371, 2014.

[119] V. Mazumder, M. Chi, K. L. More, and S. Sun, "Core/Shell Pd/FePt nanoparticles as an active and durable catalyst for the oxygen reduction reaction," *Journal of the American Chemical Society*, vol. 132, no. 23, pp. 7848–7849, 2010.